

AD-A235 613



WRDC-TR-90-2120

INVESTIGATION INTO THE FAILURE CAUSE OF A
DOUBLE ACTING, LEADING EDGE GROOVE,
TILTING PAD THRUST BEARING



Brian K. Peterson
Technology Branch
Turbine Engine Division

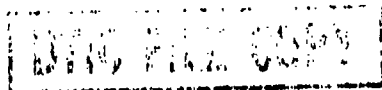
October 1990

Final Report for Period February 1990 - August 1990

Approved for public release, distribution is unlimited.

DTIC
ELECTE
MAY 13 1991
S E D

AERO PROPULSION AND POWER LABORATORY
WRIGHT RESEARCH AND DEVELOPMENT CENTER
AIR FORCE SYSTEMS COMMAND
WRIGHT-PATTERSON AIR FORCE BASE, OHIO 45433-6563



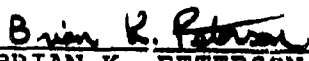
91 5 10 080


NOTICE

WHEN GOVERNMENT DRAWINGS, SPECIFICATIONS, OR OTHER DATA ARE USED FOR ANY PURPOSE OTHER THAN IN CONNECTION WITH A DEFINITELY GOVERNMENT-RELATED PROCUREMENT, THE UNITED STATES GOVERNMENT INCURS NO RESPONSIBILITY OR ANY OBLIGATION WHATSOEVER. THE FACT THAT THE GOVERNMENT MAY HAVE FORMULATED OR IN ANY WAY SUPPLIED THE SAID DRAWINGS, SPECIFICATIONS, OR OTHER DATA, IS NOT TO BE REGARDED BY IMPLICATION, OR OTHERWISE IN ANY MANNER CONSTRUED, AS LICENSING THE HOLDER, OR ANY OTHER PERSON OR CORPORATION; OR AS CONVEYING ANY RIGHTS OR PERMISSION TO MANUFACTURE, USE, OR SELL ANY PATENTED INVENTION THAT MAY IN ANY WAY BE RELATED THERETO.

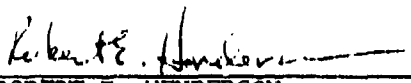
THIS REPORT HAS BEEN REVIEWED BY THE OFFICE OF PUBLIC AFFAIRS (ASD/PA) AND IS RELEASABLE TO THE NATIONAL TECHNICAL INFORMATION SERVICE (NTIS). AT NTIS IT WILL BE AVAILABLE TO THE GENERAL PUBLIC INCLUDING FOREIGN NATIONS.

THIS TECHNICAL REPORT HAS BEEN REVIEWED AND IS APPROVED FOR PUBLICATION.


BRIAN K. PETERSON
Project Engineer
Technology Branch


FRANCIS R. OSTDIEK
Chief, Technology Branch
Turbine Engine Division

FOR THE COMMANDER


ROBERT E. HENDERSON
Deputy for Technology
Turbine Engine Division
Aero Propulsion & Power Directorate

IF YOUR ADDRESS HAS CHANGED, IF YOU WISH TO BE REMOVED FROM OUR MAILING LIST, OR IF THE ADDRESSEE IS NO LONGER EMPLOYED BY YOUR ORGANIZATION PLEASE NOTIFY WL/POTX, WRIGHT-PATTERSON AFB, OH 45433-6563 TO HELP MAINTAIN A CURRENT MAILING LIST.

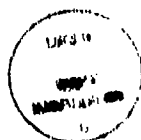
COPIES OF THIS REPORT SHOULD NOT BE RETURNED UNLESS RETURN IS REQUIRED BY SECURITY CONSIDERATIONS, CONTRACTUAL OBLIGATIONS, OR NOTICE ON A SPECIFIC DOCUMENT.

REPORT DOCUMENTATION PAGE

1a. REPORT SECURITY CLASSIFICATION Unclassified			1b. RESTRICTIVE MARKINGS N/A		
2a. SECURITY CLASSIFICATION AUTHORITY N/A			3. DISTRIBUTION/AVAILABILITY OF REPORT Approved for public release; distribution is unlimited.		
2b. DECLASSIFICATION/DOWNGRADING SCHEDULE N/A					
4. PERFORMING ORGANIZATION REPORT NUMBER(S) WRDC-TR-90-2120			5. MONITORING ORGANIZATION REPORT NUMBER(S)		
6a. NAME OF PERFORMING ORGANIZATION Aero Propulsion & Power Lab WRDC, AFSC		6b. OFFICE SYMBOL (if applicable) WRDC/POTX	7a. NAME OF MONITORING ORGANIZATION		
6c. ADDRESS (City, State, and ZIP Code) Wright-Patterson AFB OH 45433			7b. ADDRESS (City, State, and ZIP Code)		
8a. NAME OF FUNDING / SPONSORING ORGANIZATION		8b. OFFICE SYMBOL (if applicable)	9. PROCUREMENT INSTRUMENT IDENTIFICATION NUMBER		
8c. ADDRESS (City, State, and ZIP Code)			10. SOURCE OF FUNDING NUMBERS		
			PROGRAM ELEMENT NO. 63202F	PROJECT NO. 668A	TASK NO. 05
					WORK UNIT ACCESSION NO. 02
11. TITLE (Include Security Classification) Investigation into the Failure Cause of a Double Acting, Leading Edge Groove, Tilting Pad Thrust Bearing					
12. PERSONAL AUTHOR(S) Brian K. Peterson					
13a. TYPE OF REPORT Final		13b. TIME COVERED FROM 2/90 TO 8/90		14. DATE OF REPORT (Year, Month, Day) October 1990	
15. PAGE COUNT 56					
16. SUPPLEMENTARY NOTATION N/A					
17. COSATI CODES			18. SUBJECT TERMS (Continue on reverse if necessary and identify by block number)		
FIELD	GROUP	SUB-GROUP	Bearing, Thrust Bearing, Tilting Pad Galling		
			Friction Abrasion Lubrication		
			Titanium Adhesion		
19. ABSTRACT (Continue on reverse if necessary and identify by block number) This report describes the results of bench tests simulating operation and failure of a thrust bearing used in a gas turbine engine compressor development test rig. The bearing was a double acting, tilting pad with offset pivot, leading edge groove configuration using an AMS 4928 titanium collar and C18200 copper-chrome alloy pads with a No. 2 babbitt face. The bench tests successfully simulated the bearing failure and demonstrated a materials incompatibility. This was supported by visual examination, scanning electron microscopy and X-ray energy spectroscopy. A comparison of the bench test results to the compressor rig bearing failure is provided to support the report conclusions.					
20. DISTRIBUTION/AVAILABILITY OF ABSTRACT <input checked="" type="checkbox"/> UNCLASSIFIED/UNLIMITED <input type="checkbox"/> SAME AS RPT. <input type="checkbox"/> DTIC USERS			21. ABSTRACT SECURITY CLASSIFICATION Unclassified		
22a. NAME OF RESPONSIBLE INDIVIDUAL BRIAN K. PETERSON			22b. TELEPHONE (Include Area Code) 513/255-4141		22c. OFFICE SYMBOL WRDC/POTX

PREFACE

This report was prepared by Mr. Brian K. Peterson of the Technology Branch, Turbine Engine Division, Aero Propulsion and Power Laboratory, Wright Research and Development Center, Wright-Patterson AFB, Ohio. The work was accomplished between 1 February 1990 and 31 August 1990. This report represents results from a portion of the effort of the Compressor Research Facility (CRF) and was conducted under Work Unit XX, Task XX, of Project XXXX, "CRF XTE-65 Test Program."



Accession For	
NTIS GRA&I	<input checked="" type="checkbox"/>
DTIC TAB	<input type="checkbox"/>
Unannounced	<input type="checkbox"/>
Justification	
By	
Distribution/	
Availability Codes	
Dist	Avail and/or Special
A-1	

TABLE OF CONTENTS

SECTION	PAGE
I INTRODUCTION	1
II BACKGROUND	2
III BENCH TESTING	3
A. Materials and Lubricant	3
B. Test Apparatus and Instrumentation	4
C. Experimental Procedures	4
IV RESULTS	8
A. Compressor Bearing Failure	8
B. Bench Test Results	14
1. Bench Test 1	14
a. Test Data	14
(1) Test Segments I and II	14
(2) Test Segments III and IV	14
b. Visual Examination	18
c. SEM and X-Ray Spectroscopy Results	19
2. Bench Test 2	29
3. Bench Test 3	29
a. Test Data	29
b. Visual Examination	32
c. SEM and X-Ray Spectroscopy Results	32
V DISCUSSION	41
A. Comparison of Compressor Bearing Failure and Bench Test Results	41
B. Failure Sequence	42
C. Supporting Evidence	42
VI CONCLUSIONS	45
VII RECOMMENDATIONS	46
VIII ACKNOWLEDGEMENTS	47
IX REFERENCES	48

LIST OF FIGURES

FIGURE	PAGE
3.1 Test Setup - Bench Test 1	5
3.2 Test Setup - Bench Test 2	5
4.1 Forward Compressor Bearing	9
4.2 Rear Compressor Bearing Pad	10
4.3 Compressor Bearing Collar	11-12
a. Forward Face	11
b. Rear Face	12
4.4 Compressor Bearing Speed and Temperature	13
a. Speed vs. Time	13
b. Temperature - Forward Pads 1, 2 and 3	13
c. Temperature - Forward Pads 4, 7, 11	13
d. Temperature - Rear Pads 1 and 2	13
4.5 Compressive Load Cell Results - Bench Test 1	15
4.6 Compressive Load Cell Results - Test Segments I and II	15
4.7 Compressive Load Cell Results - Test Segment III	16
a. Test Segment IIIa	16
b. Test Segment IIIb	16
4.8 Compressive Load Cell Results - Test Segment IV	17
a. Compressive Load Cell Results - Test Segment IV	17
b. Compressive Load Cell Results - First 37 Seconds of Test Segment IV	17
4.9 Temperature Results - Bench Test 1	19
a. Thermocouple 1	19
b. Thermocouple 2	19
c. Thermocouple 4	19
4.10 Bearing Pad Photographs	20-22
a. After Test Segment IIIa	20
b. After Test Segment IIIb	21
c. After Test Segment IV	22
4.11 Collar and Pad After Bench Test 1	23
4.12 SEM Photograph of Pad After Bench Test 1	23

4.13 SEM Photographs of Pad After Bench Test 1	24-28
a. Smeared Failure Zone	24
b. Smeared Failure Zone	25
c. Galled Failure Zone	26
d. Foreign Particle Damage	27
e. Abrasive Wear Track	28
4.14 Load Cell Results - Bench Test 2	30
4.15 Fluid Film Development - Bench Test 2	30
4.16 Thermocouple Results - Bench Test 2	31
a. Thermocouple 1	31
b. Thermocouple 2	31
c. Thermocouple 3	31
d. Thermocouple 4	31
4.17 Compressive Load Results - Bench Test 3	33
4.18 Friction Load Results - Bench Test 3	33
4.19 Friction Coefficient vs. Time - Bench Test 3	34
4.20 Bearing Pad After Bench Test 3	35
4.21 Bearing Pad and Collar After Bench Test 3	36
4.22 SEM Photographs of Pad After Bench Test 3	38-40
a. Wear Scar Beginning	38
b. Wear Scar Beginning - Smeared Zone	38
c. Wear Scar Beginning - Galled Zone	39
d. Wear Scar Exit	40
e. Wear Scar Exit - Galled Zone	40

LIST OF TABLES

TABLE	PAGE
3.1 Test Sequence	6
4.1 Compressor Bearing Failure Oil Analysis Results	8

I. INTRODUCTION

Upon commercial development in the 1950's, titanium alloys were investigated for numerous applications because of high strength to weight ratio titanium offered. Early work, including sliding tests by Rabinowicz¹ identified poor frictional properties associated with titanium and the early titanium alloys. These properties included the tendency to gall and an inability to react with most lubricants.

The tendency of titanium to adhere to other metals has been explained by solid-phase welding². This is further complicated by the inability of titanium oxides on the surface to chemically react with ordinary lubricants, allowing metal to metal contact in friction reduction applications. To date, efforts to reduce friction and the galling and seizing of bare titanium surfaces have been unsuccessful with almost all combinations of metals and lubricants.

It is the purpose of this paper to show the disastrous results of using Ti 6-4 alloy against babbit No. 2 in a bearing design and provide some insight into the wear mechanisms present.

II. BACKGROUND

This study was undertaken in an effort to determine the cause of the failure of a double acting, tilting pad thrust bearing with leading edge grooves and offset pivot. The bearing was designed to carry the thrust load of a gas turbine engine fan compressor during development testing in the Compressor Research Facility (CRF) of the Wright Research and Development Center. The bearing failed after 9 hours, 14 minutes of operation above minimum speed (approximately 3500 rpm). The potential impact to an important and tightly scheduled development test demanded a quick solution to the problem.

The thrust collar was constructed of annealed AMS 4928 titanium alloy with a surface finish of 5-10 μ in. Sixteen bearing pads were constructed of C18200 copper-chrome alloy base with a No. 2 babbitt face, eight placed on either side of the thrust collar to transmit loads in both axial directions. The forward pads transmitted the thrust load of the compressor and the rear pads transmitted any reverse loads owing to reverse flow conditions or vibration. Lubrication was Mobil DTE-797 oil supplied under pressure to the leading-edge groove of each pad. The leading-edge groove is a slot in each bearing pad used to introduce the lubricant between the surfaces. Bearing operation was typified by two regimes; low speed, low load operation during start-up; and, high speed, high load operation during compressor testing.

III. BENCH TESTING

In order to quickly determine the cause of failure, a bench test of the bearing was designed and conducted to duplicate the failure. Thermocouples located in the pads of the failed compressor bearing indicated increased bearing stress during low speed operation. Based on this evidence, bench testing was designed to simulate the low speed operating regime.

Three bench tests were conducted. The purpose of the first was to duplicate and observe the compressor bearing failure to arrive at an immediate solution. The second bench test was conducted to verify that the experimental setup and procedures did not effect the results of the first bench test. The third bench test stopped the test at failure initiation to describe the initial wear mechanism.

A. Materials and Lubricant

The materials and lubricant used in bench testing were chosen to simulate the compressor bearing. Some features of the compressor bearing could not be simulated and will be discussed later in the report. The effects of these features on the simulation results were considered minimal because of the low loads and speeds tested.

The first bench test used the same titanium collar which failed in the compressor, restored to its original surface finish. The bearing pad was constructed of the same materials as those used in the compressor bearing. The pad had a central pivot and there was no leading edge groove.

The second bench test used an annealed AMS 4140 steel thrust collar. The bearing pad used was identical to the one used in the first bench test.

The third bench test used the opposite face of the titanium thrust collar. The bearing pad was identical to the two used in the previous bench tests except for the use of annealed AISI 1020 steel as a base material.

Lubrication for all bench tests was the same as that used in the compressor bearing, Mobil DTE-797. Since no leading edge groove and no pressurized source of oil was available, lubricant was provided by gravity feed to the leading edge of the bearing pad in each bench test. Since the bearing was in boundary lubrication at low speeds, the effect of the change in lubrication methods was expected to be minimal. Flow was sufficient to provide an overflow of lubricant at the pad leading edge. The similarity of the bearing pad and thrust collar after the bench tests to the pad and thrust collar of the failed compressor bearing seemed to confirm that the effect of this difference was minimal.

B. Test Apparatus and Instrumentation

The test apparatus used in the first two bench tests is illustrated in Figure 3.1. The titanium and steel collars were mounted in a gear-driven machinists lathe. The collar face was trued to within 0.0005 inches. A steel mounting fixture was constructed for holding a single bearing pad. The fixture used eight pins to hold the pad in place while still allowing the pad to pivot. The mounting fixture was attached to a 2000-lb capacity load cell used to monitor the simulated thrust load. The load cell was mounted to the lathe tool holder which provided a stable platform that could be moved into place to apply the load. A digital voltmeter was used to monitor the static load during application.

The test apparatus was slightly modified for the third bench test. A schematic drawing showing the changes can be seen in Figure 3.2. A second load cell was mounted below the bearing pad for measurement of the friction load. The bottom mounting fixture pins were removed and a single vertical pin was used to transmit the frictional load from the pad to the additional load cell. To account for any friction force transmitted through the pivot point, a cantilever beam was instrumented with strain gages to monitor any force in the direction of the frictional load. Moments generated by the frictional force, because of the variation of friction with radial location, were not monitored.

The pads used in the first and second bench tests were instrumented with four thermocouples each. These were placed in central locations to provide transient pad temperature data throughout the test. The pad used during the third bench test was not instrumented with thermocouples.

Lubricant was supplied using gravity feed from a tank mounted above the lathe. The setup provided 1.7 gallons per hour during the first two bench tests. A filter was added to the oil supply during the third bench test to eliminate the possibility of contamination. This reduced the flow rate to 1.2 gallons per hour.

Data were recorded using an FM instrumentation tape recorder. An oscillograph was used to allow monitoring of the load and temperatures during testing.

C. Experimental Procedures

The bench tests were completed following the experimental procedures listed below.

1. A static load was applied in accordance with the schedule shown in Table I.

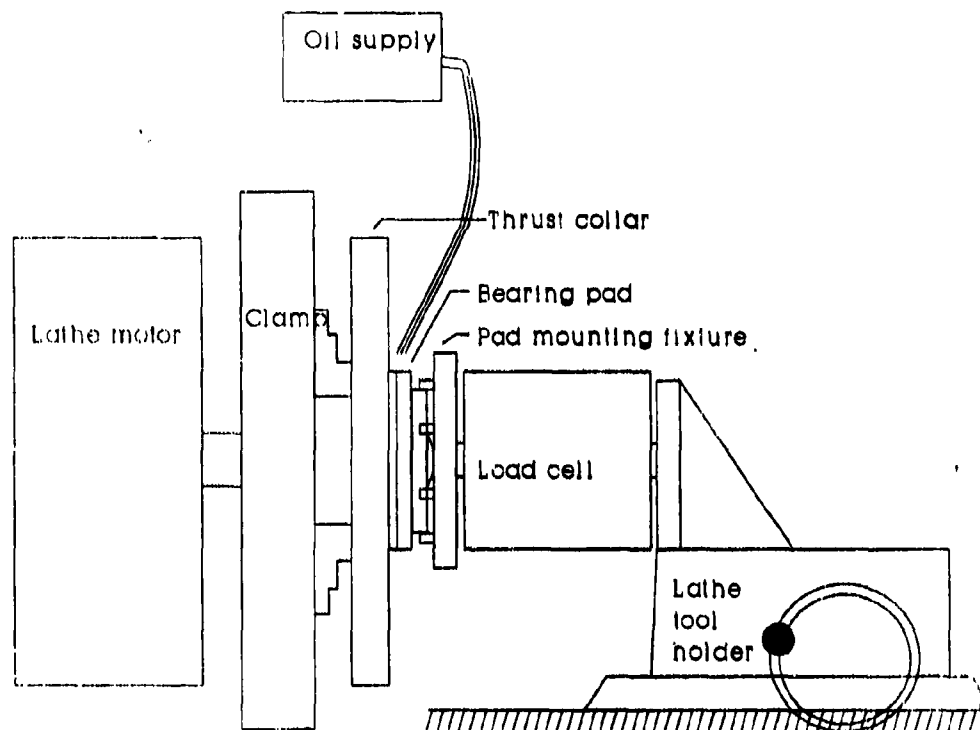


Figure 3.1 Test Setup - Bench Test 1

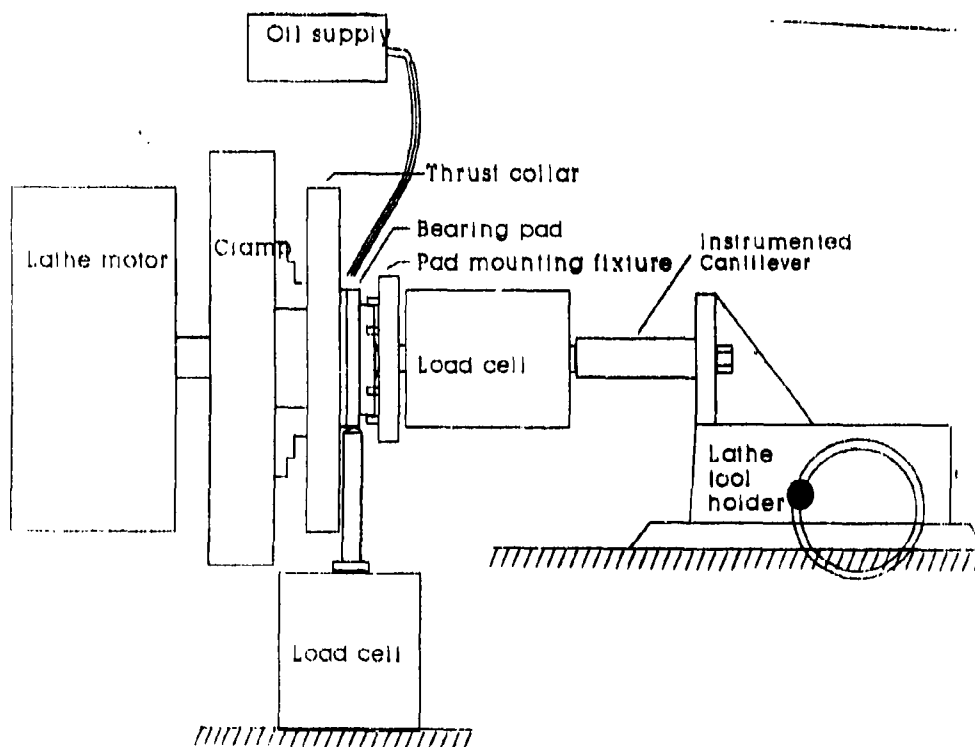


Figure 3.2 Test Setup - Bench Test 2

Table I Test Sequence

Test Segment	Bench Test	Load (pounds)	Time (min.)	Speed (rpm)	Collar Material	Pad Material
I	1	0	5	9.3	Ti	Cu
II	1	100	5	9.3	Ti	Cu
III	1	200-800	5	9.3	Ti	Cu
IV	1	25	15	146.0	Ti	Cu
V	2	0	5	9.3	Steel	Cu
VI	2	100	5	9.3	Steel	Cu
VII	2	200	5	9.3	Steel	Cu
VIII	2	500	5	9.3	Steel	Cu
IX	2	25	15	146.0	Steel	Cu
X	2	500	15	146.0	Steel	Cu
XI	3	25	3	9.3	Ti	Steel

2. Lubricant flow was started and all air was cleared from the oil supply line.

3. Following assurance that the bearing leading edge was fully wetted, the collar was rotated at the scheduled speed listed in Table I.

4. Oil samples were taken during each bench test.

5. Each test segment was halted after the time specified in Table I had elapsed.

6. The pad and collar were visually examined only at the end of test segments identified in Table I.

7. The next scheduled static load was applied and the process repeated. Testing was halted when the desired amount of bearing damage had occurred or when the schedule time had elapsed.

Following completion of bench tests 1 and 3, a thorough examination of pad and collar surfaces was completed. Examination of the pad and collar used in bench test 2 was not conducted since no relevant information was expected. This examination was conducted in the order listed below.

1. Visual and microscopic examination of both surfaces was completed.

2. Scanning electron microscopy and X-ray spectroscopic examination of babbitt surface samples was completed.

3. X-ray spectroscopic examination of collar surface samples was completed in bench test 1. Samples of the collar surface were not attainable in bench test 3.

IV. RESULTS

A. Compressor Bearing Failure

As shown in Figure 4.1, damage to the forward bearing pads was extensive, resulting in the complete loss of babbitt material on all bearing pads and destruction of all evidence of the failure cause. More information on the failure cause was available from the rear pads. Evidence of scoring and galling was apparent on the rear pads shown in Figure 4.2. Scoring is evident on the forward and rear sides of the titanium thrust collar as shown in Figures 4.3a and 4.3b, respectively.

Thermocouples in the forward and rear bearing pads indicated elevated temperatures and increased bearing stress during compressor start, followed by reduced temperatures occurring when the compressor was throttled above starting speed. This is best illustrated during the first start of the compressor. Plots of speed vs. time and bearing pad temperatures vs. time during the first start are provided in Figure 4.4. Increased bearing stress was observed on both front and rear bearing pads.

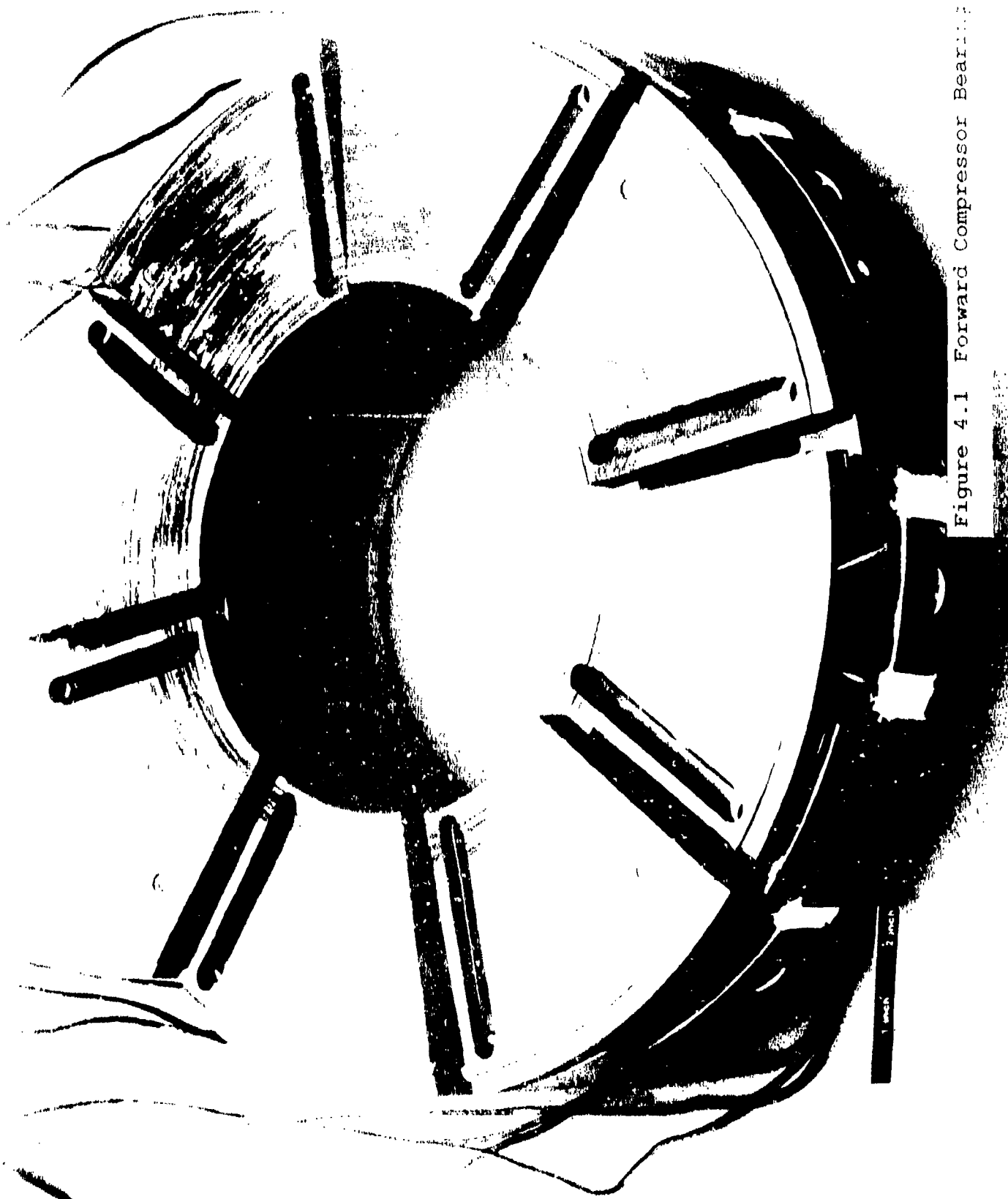
Scavenge oil samples were taken after the failure at two locations in the oil scavenge system. One was taken aft of a 40-micron filter, and another was taken aft of a 20-micron filter. Table II presents the results of both samples. The bearing oil supply was common with the lubrication system of the CRF drive lube oil system, providing a second source of debris. Large amounts of bearing debris were evident in the sample.

Table II Compressor Bearing Failure Oil Analysis Results

Sample/ Filter Size (microns)	Fe	Ag	Al	Cr	Cu	Mg	Ni	Pb	Si	Sn	Ti
1/40	0	0	0	0	0	0	0	0	1.3	0	0
2/20	480	0.4	274	8.5	252	2.6	13.8	44.3	14.1	998	998

X-ray spectroscopy examination of the surface of a rear pad was completed by the contractor who designed the compressor. This revealed, in order of descending amounts, the presence of carbon, chlorine, tin, titanium, sulfur, sodium, aluminum, and oxygen.

Figure 4.1 Forward Compressor Bearing



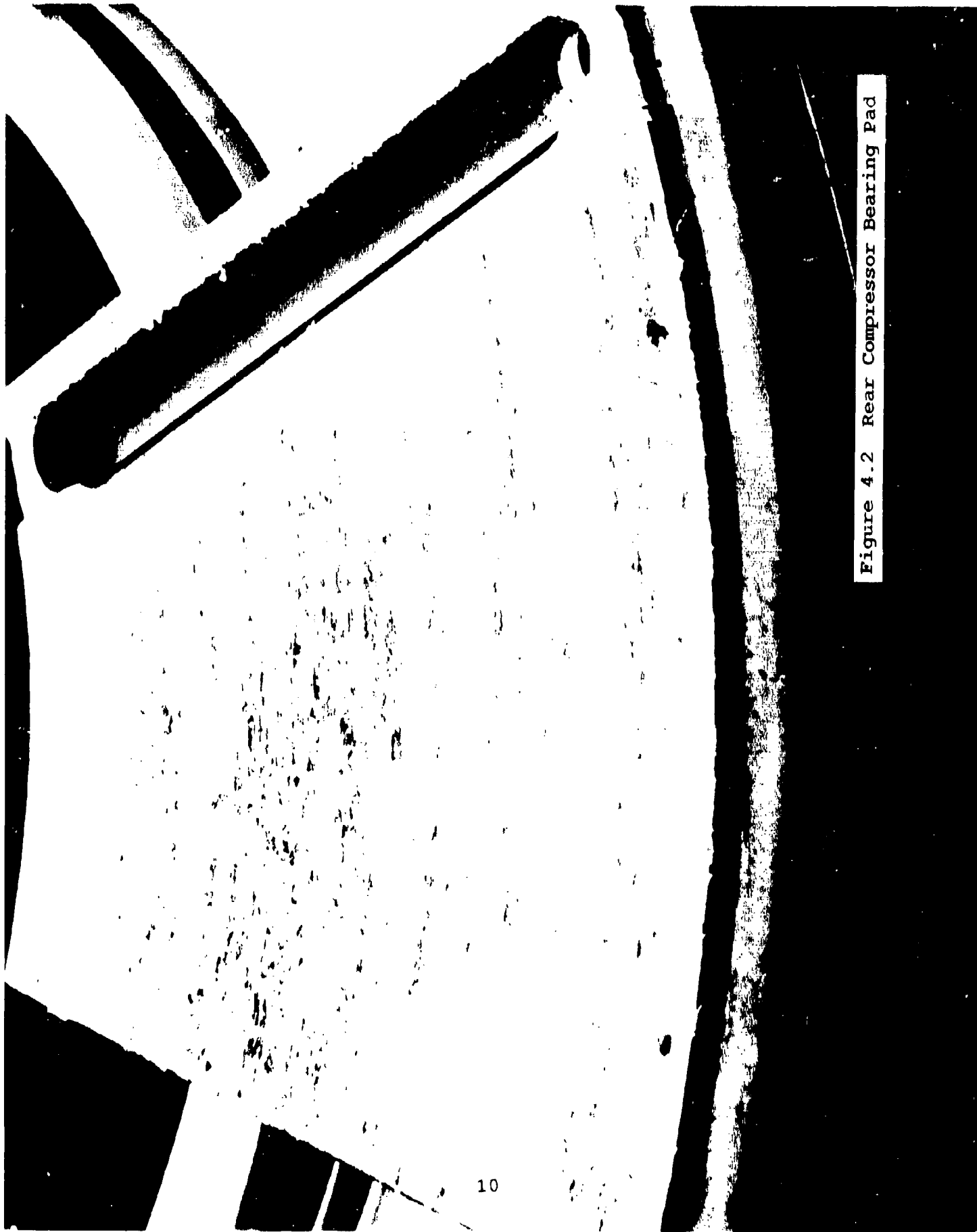


Figure 4.2 Rear Compressor Bearing Pad

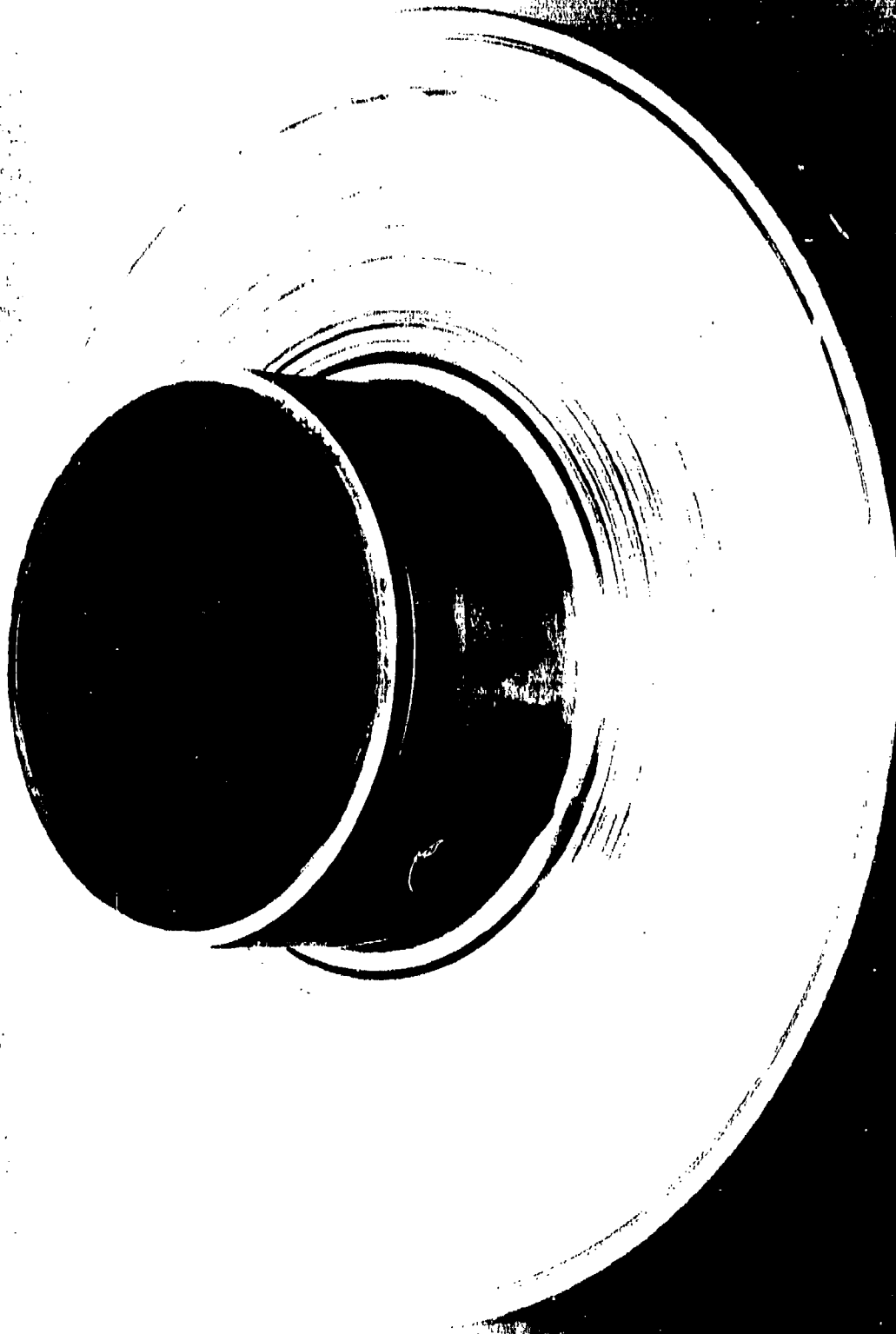


Figure 4.3a

Compressor Bearing Collar

Forward Face

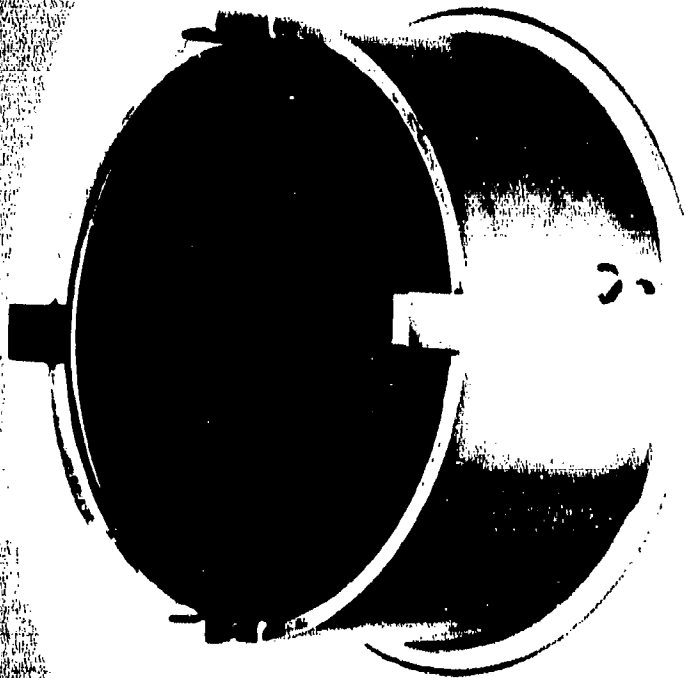


Figure 4.3b

Compressor Bearing Collar

Rear Face

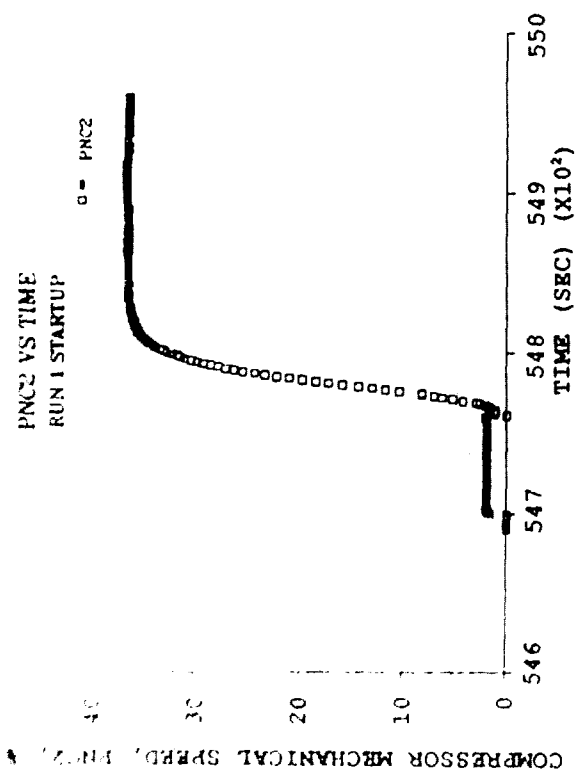


Figure 4.4a Speed vs. Time

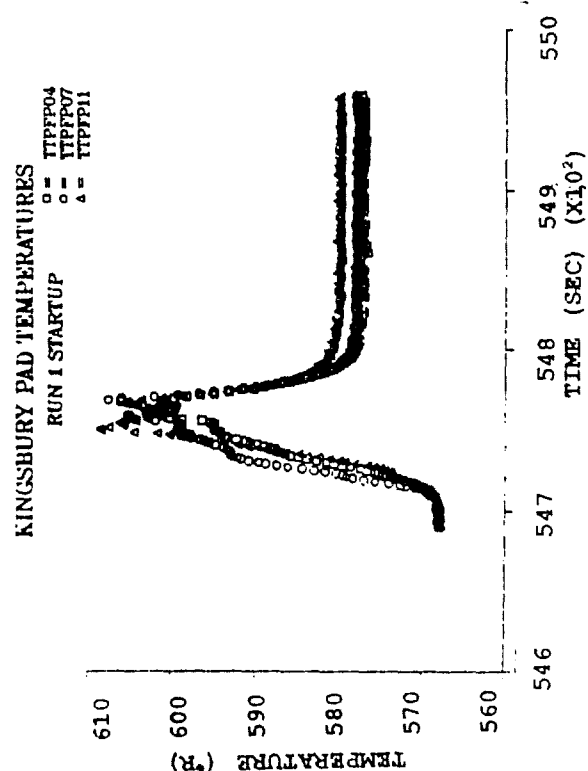


Figure 4.4c Temperature - Forward Pads

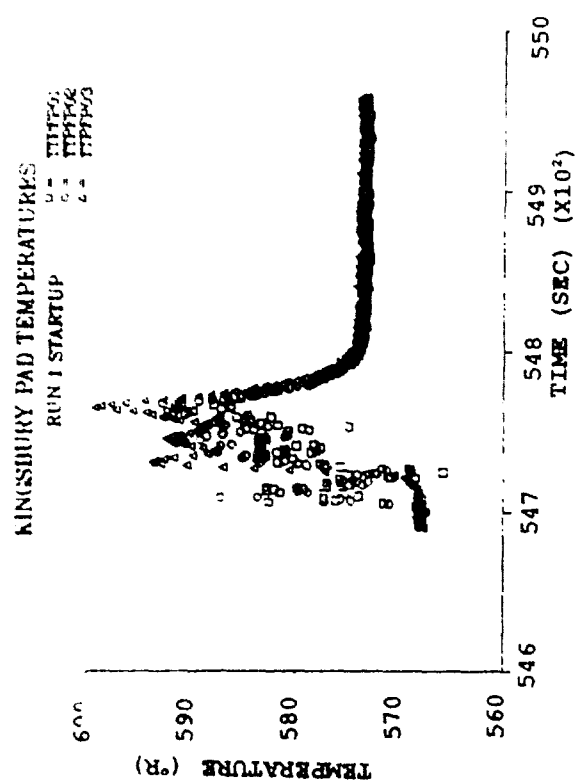


Figure 4.4b Temperature - Forward Pads

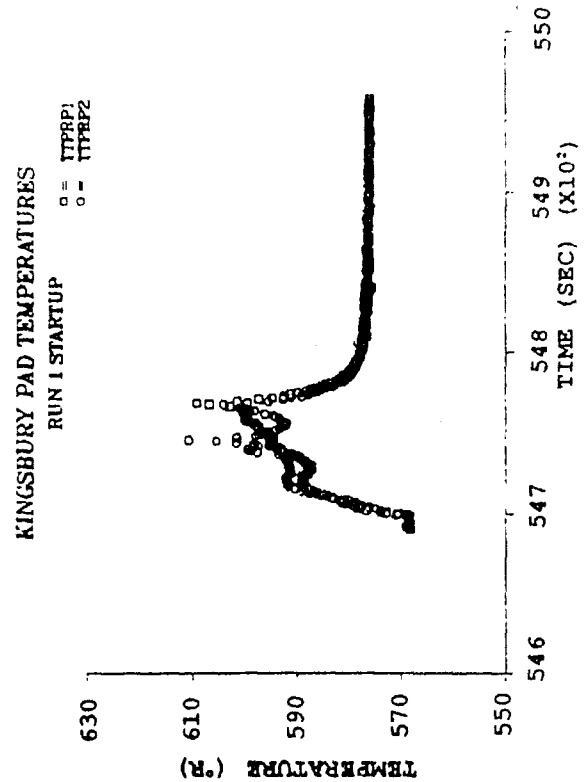


Figure 4.4d Temperature - Rear Pads 1 and 2

Figure 4.4 Compressor Bearing Speed and Temperature

B. Bench Test Results

1. Bench Test 1

Bench test 1 was allowed to progress past failure initiation. Failure was defined as the breakdown of the bearing surfaces. The primary objective of the test was to duplicate the failure of the bearing to verify the theory of material incompatibility as the cause of the failure.

a. Test Data Results from the load cell measuring compressive load are presented in Figure 4.5. Each of the test segments listed in Table 1 are labeled in Figure 4.5.

(1) Test Segments I and II Load cell data from test segments I and II are presented in Figure 4.6. These results show a cyclic loading present in all the data taken. The frequency of the cyclic loading is the same as the frequency of the rotating collar, indicating that it is due to the runout of the collar. The cyclic loading was not of sufficient magnitude and duration to cause fatigue of the babbitt. This was proven later during the third bench test when examination of the cross section of a failed area revealed no subsurface cracking.

(2) Test Segments III and IV Test segment III was divided into two portions, IIIa and IIIb, and is presented in Figures 4.7a and 4.7b. After approximately 20 seconds into segment III, enough torque was generated to turn the bearing pad slightly. The torque was caused by the radial variations in frictional load because of the change in thrust collar velocity and the distance slid with radial location. The test was halted and a stop was added to counteract the torque. Testing was restarted and the load cycle magnitude increased because of an increased offset in the thrust collar runout. Test segment III was not of sufficient duration to initiate babbitt fatigue.

Load cell results from test segment IV are presented in Figures 4.8a and 4.8b. Bearing failure progressed rapidly during test segment IV because of the increased rotational speed and corresponding increased distance slid. Figure 4.8a presents the load cell data taken throughout test segment IV. Figure 4.8b presents the load cell data of the first 37 seconds of test segment IV. These figures show cyclic loading at three different frequencies. The most evident is the load cycle because of slight offset in the collar face runout, which has the highest frequency. The other two cycles do not have a constant frequency. The cyclic loading of the lowest magnitude frequency is evident in Figure 4.8a and is due to the clearing and generation of wear debris. The cyclic loading with the middle frequency is most visible in Figure 4.8b. Close examination of Figure 4.7b reveals that a frequency of the same order of magnitude was present

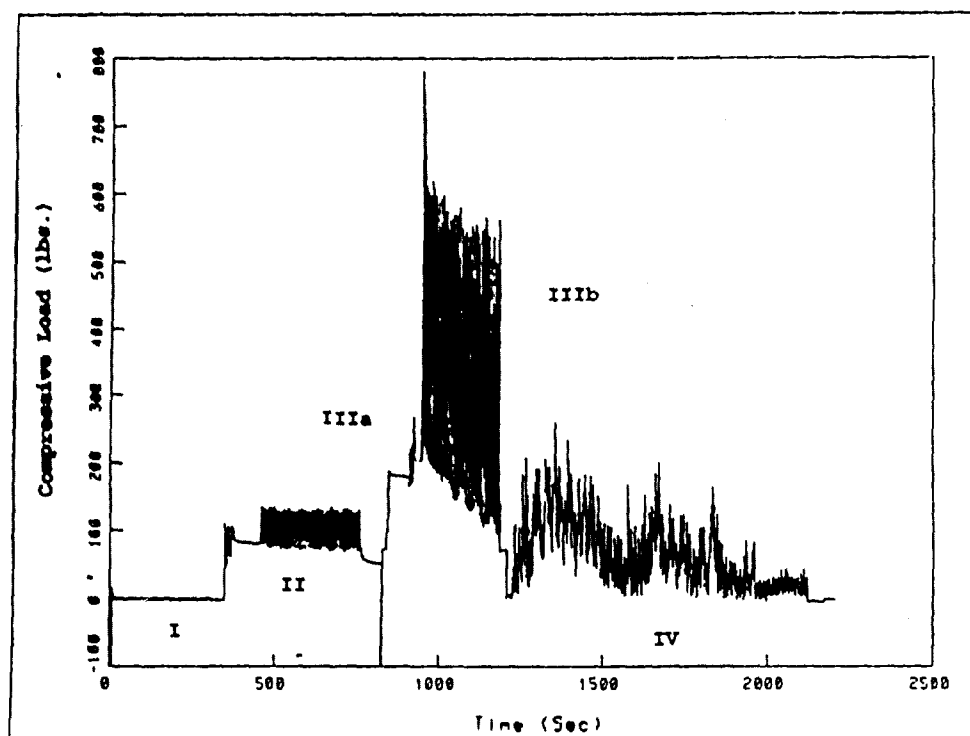


Figure 4.5 Compressive Load Cell Results - Bench Test 1

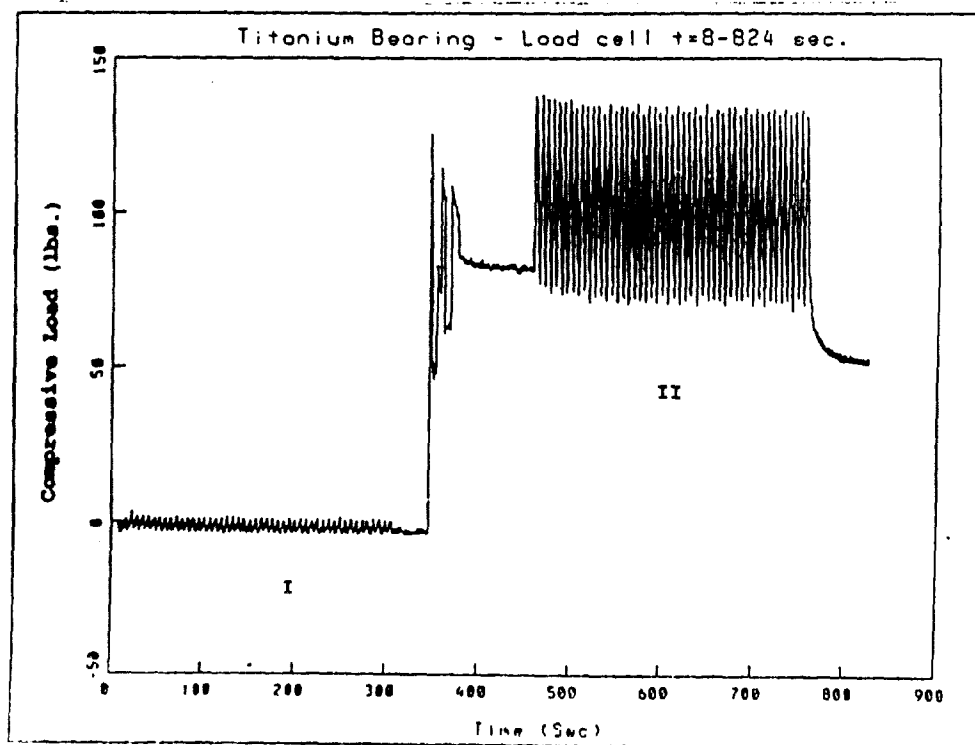


Figure 4.6 Compressive Load Cell Results
Test Segments I and II

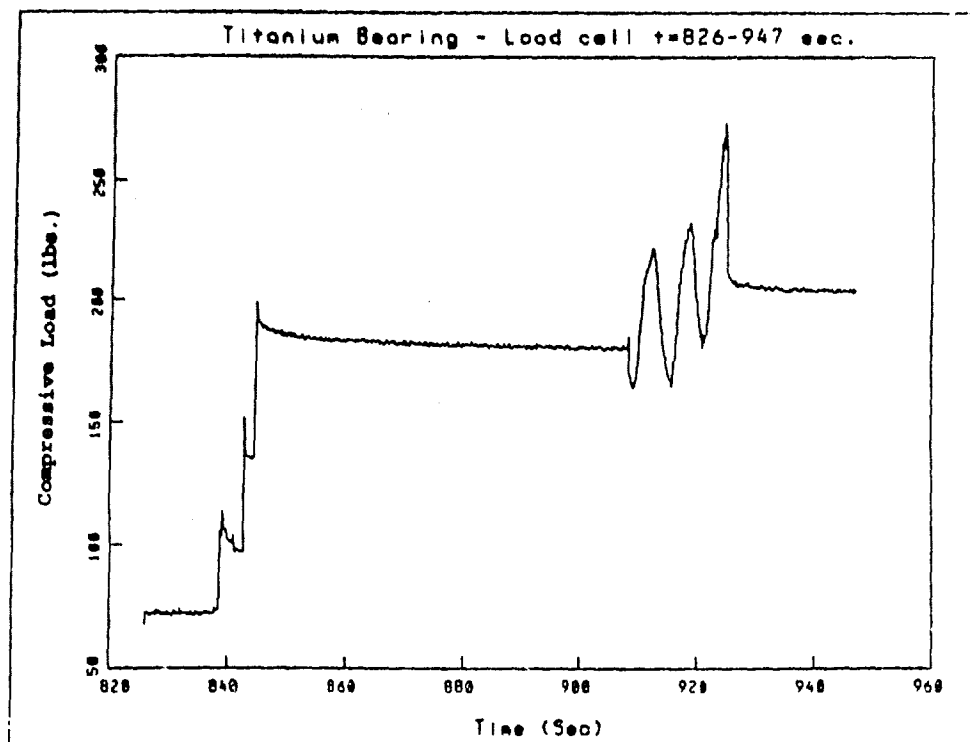


Figure 4.7a Test Segment IIIa

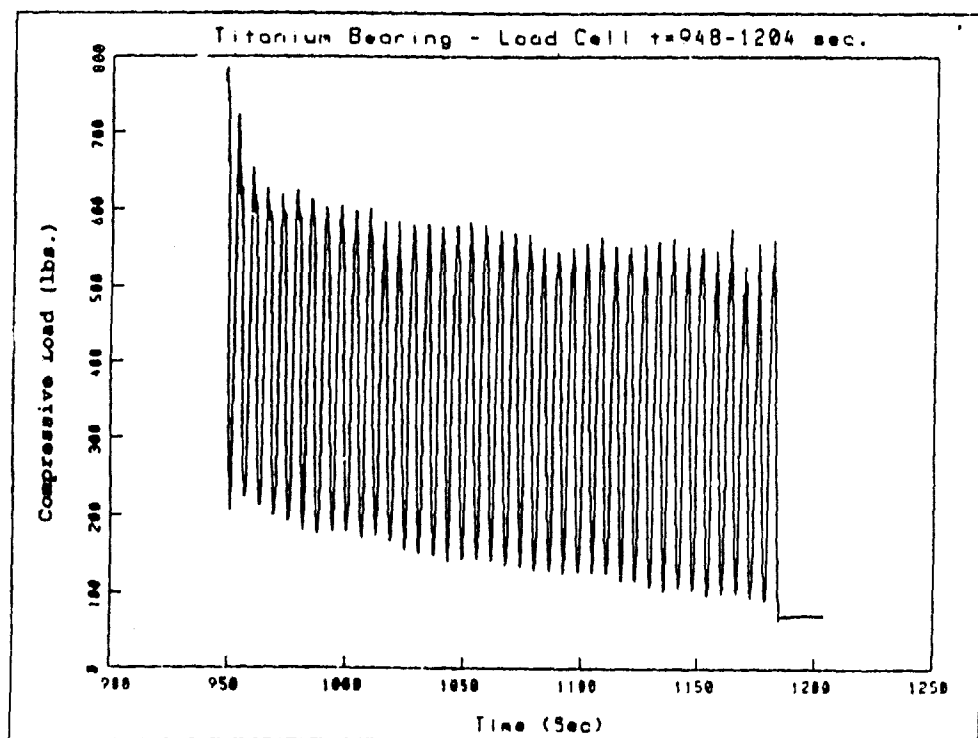


Figure 4.7b Test Segment IIIb

Figure 4.7 Compressive Load Cell Results - Test Segment III

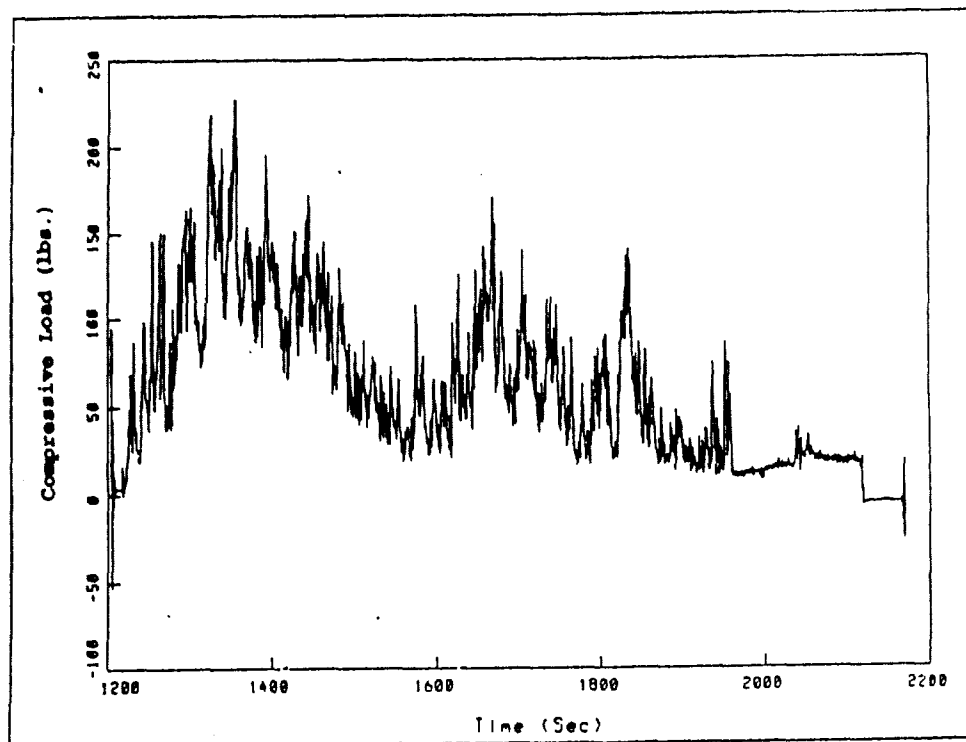


Figure 4.8a Compressive Load Cell Results
Test Segment IV

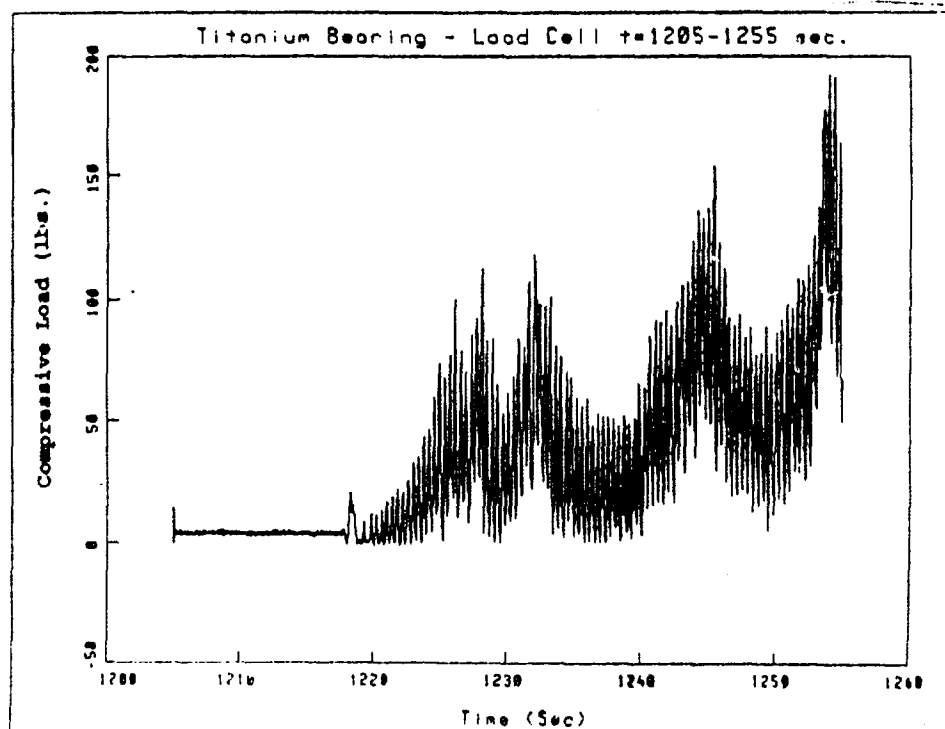


Figure 4.8b Compressive Load Cell Results
First 37 Seconds of Test Segment IV

Figure 4.8 Compressive Load Cell Results - Test Segment IV

during test segment IIIB.

Thermocouple results from bench test 1 are presented in Figure 4.9. One thermocouple failed prior to testing. Elevated bearing temperatures did not occur until test segment IIIB when galling occurred.

b. Visual Examination Figure 4.10 shows the bearing pad surfaces after various test segments. Figure 4.10a shows the pad after test segment IIIa. The black scars evident near the leading edge of the pad are the first indication of failure. The scars deviated both below and above this path of rotation. This cannot be an effect of the torque induced rotation of the pad which occurred just prior to this photograph. If it were, the scars would deviate only above the path of rotation, based on the direction of the torque induced pad rotation. No abrasion by wear particles had occurred at this point.

Figure 4.10b shows the pad after test segment IIIB. The scars evident in Figure 4.10a had grown longer and were deeper. New scars developed. Wiping and abrasion was visible behind the scars.

Figure 4.10c shows the pad after test segment IV, the completion of bench test 1. Three distinct failure modes are visible - galling, smearing, and gouging. Galling was indicated by the severe pitting. Visual examination showed wire wooling strands of copper caught in the galled areas.

Figure 4.11 shows the titanium collar next to the bearing pad. The collar exhibited deep, circumferential wear grooves. The collar surface revealed small, raised oval and rectangular shaped surfaces, approximately 0.005 by 0.020 inches in size. A sample of these was scraped off of the collar surface and the composition was determined to be primarily tin, with traces of titanium and aluminum.

c. SEM and X-Ray Spectroscopy Results Scanning electron microscopy results are presented in Figures 4.12 and 4.13. Figure 4.12 provides a 10X view of a section removed from the bearing pad. Heavy smearing, galling, and abrasion are present.

Figure 4.13 provides a closer look at some areas in Figure 4.12, as well as element identification of the surfaces. Figure 4.13a shows one of the heavily smeared areas. X-ray diffraction results show a large titanium peak, as well as tin, aluminum, silicon, and copper peaks. Figure 4.13b shows one of the flaked areas. Again, a large titanium peak is evident, along with tin, aluminum, silicon, and copper peaks. The bottom, left corner of Figure 4.13b shows a pit created by galling. Figure 4.13c is a photograph of this area. The magnification reading and scale printed on the photo should be disregarded. Titanium is the predominant peak of the element identification.

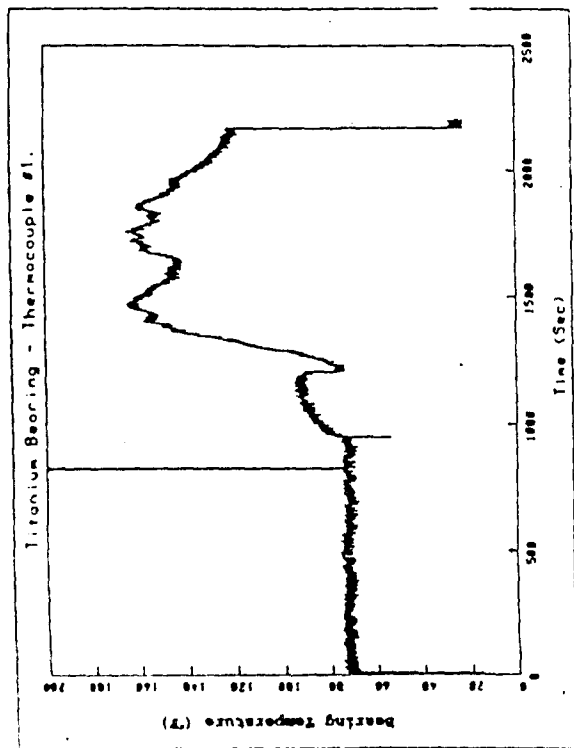


Figure 4.9a Thermocouple 1

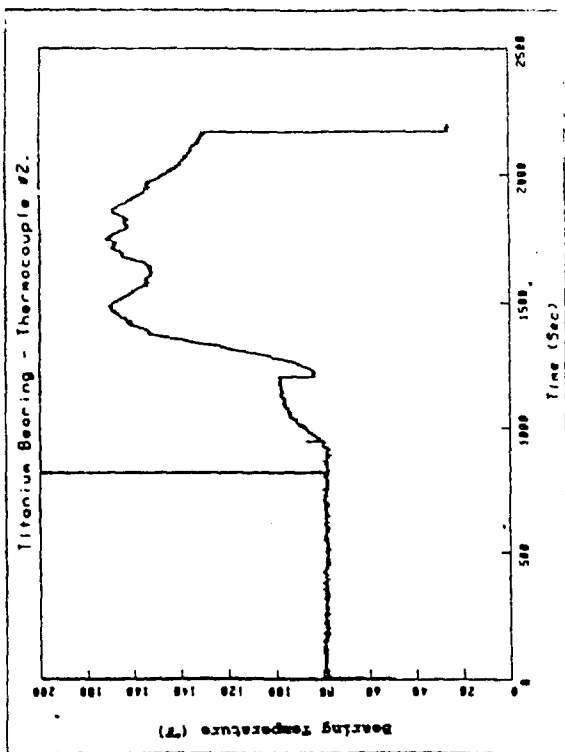


Figure 4.9b Thermocouple 2

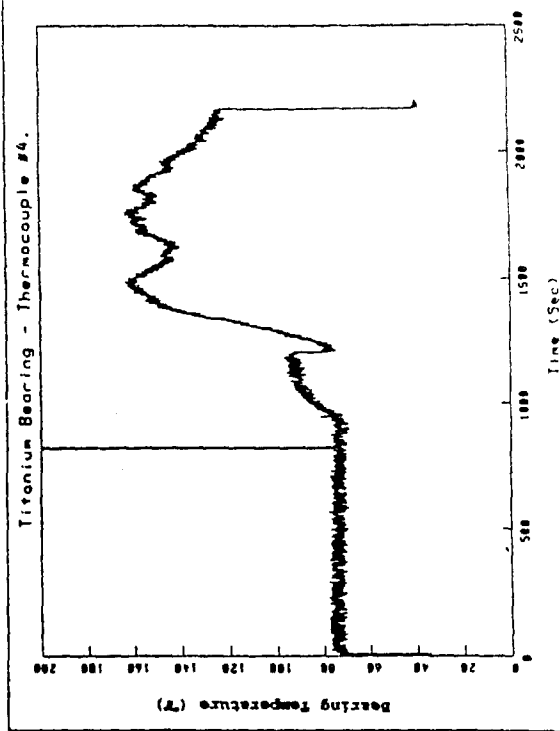


Figure 4.9c Thermocouple 4

Figure 4.9 Temperature Results - Bench Test 1




Figure 4.10a
Bearing Pad
After Test Segment IIIa

Figure 4.10b
Bearing Pad
After Test Segment 1111





Figure 4.10c

Bearing Pad

After Test Segment IV

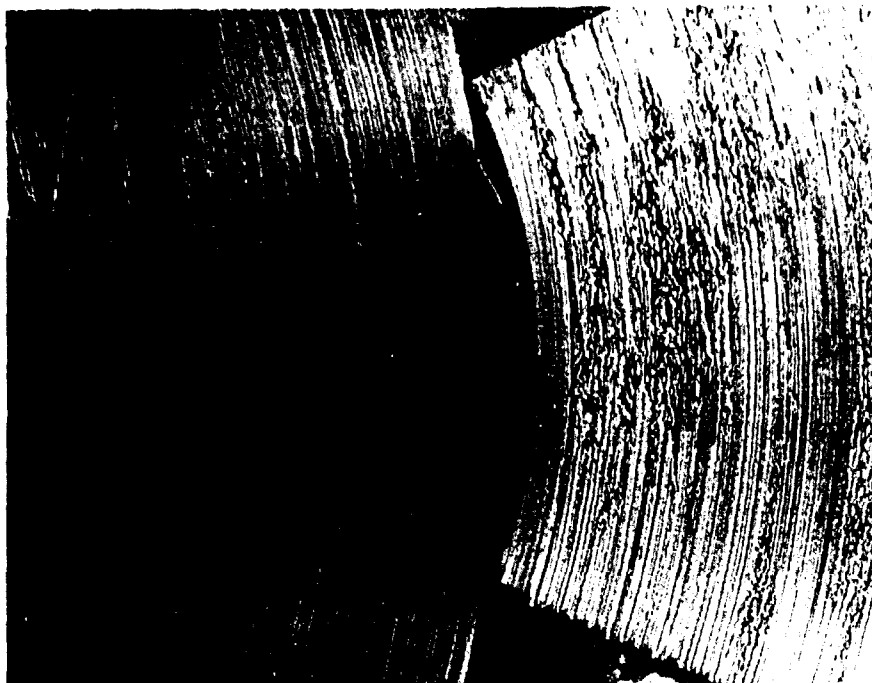


Figure 4.11 Collar and Pad After Bench Test_1

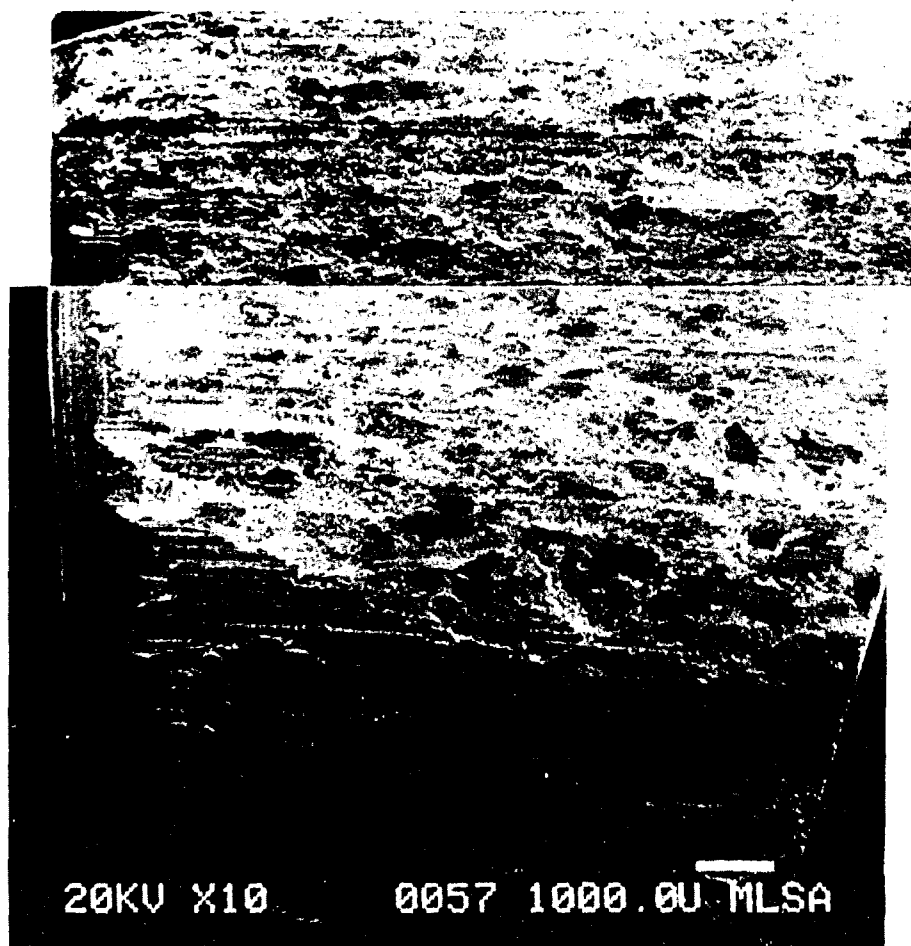


Figure 4.12 SEM Photograph of Pad After Bench Test 1



Figure 4.13 SEM Photographs of Pad
After Bench Test 1

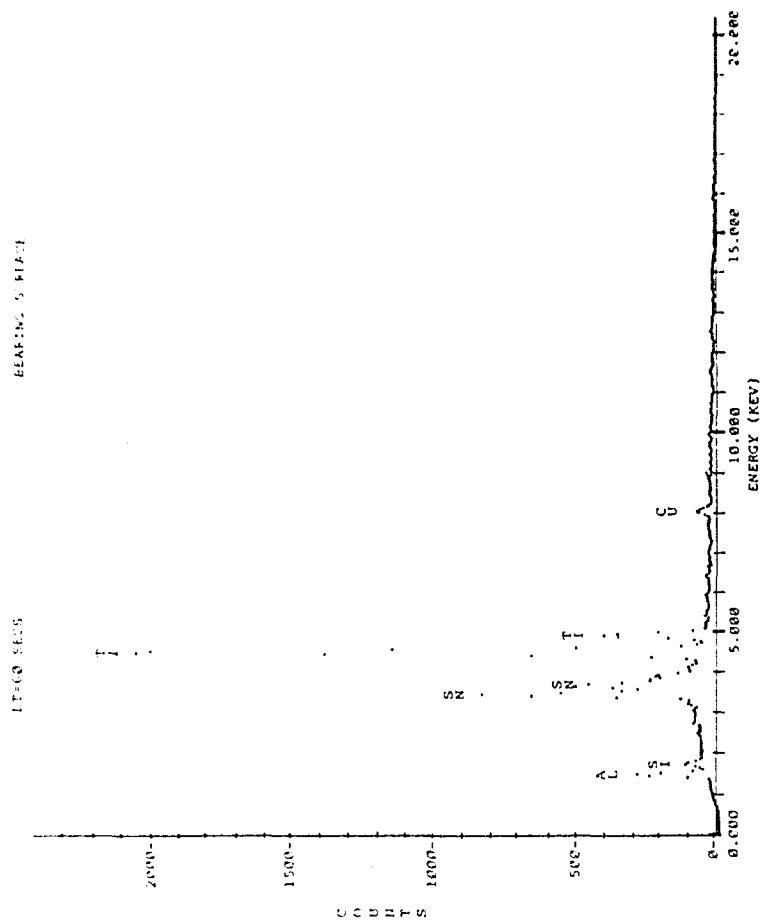


Figure 4.13a Smeared Failure Zone

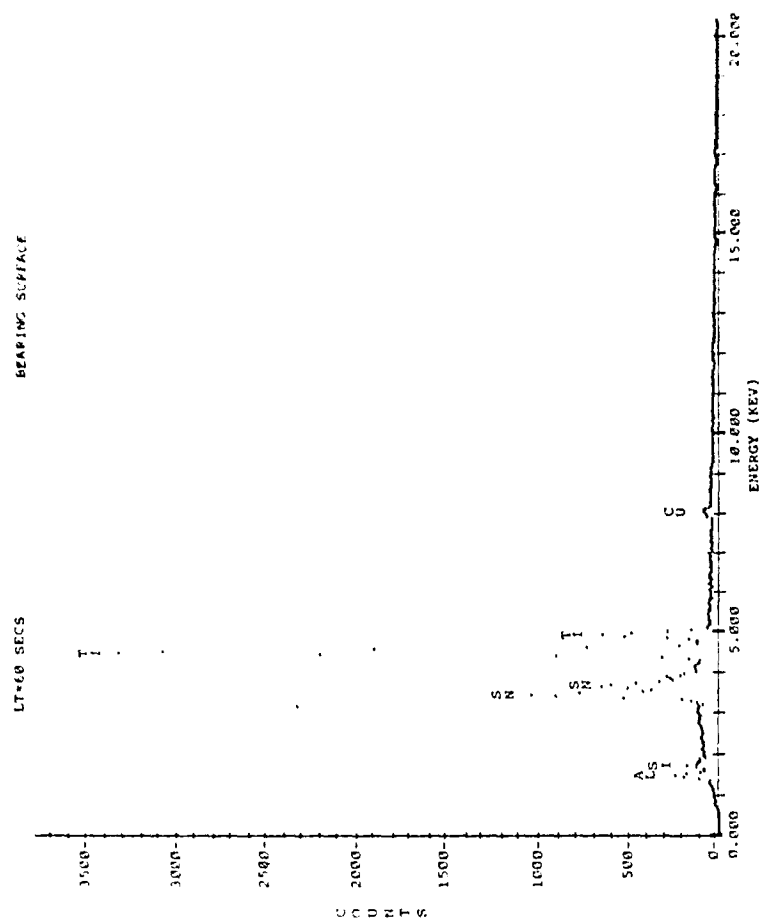
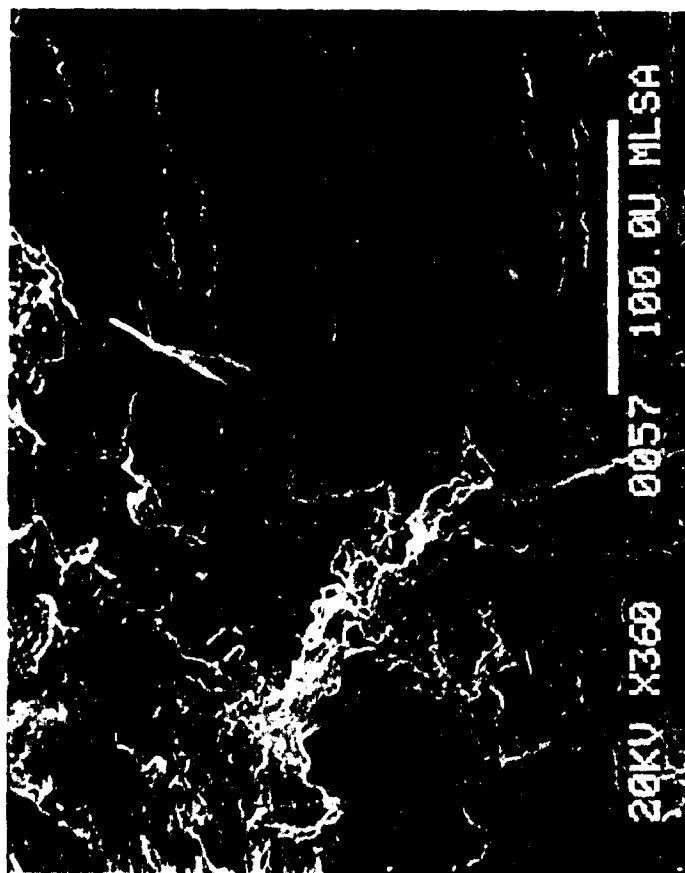


Figure 4.13b Smeared Failure Zone

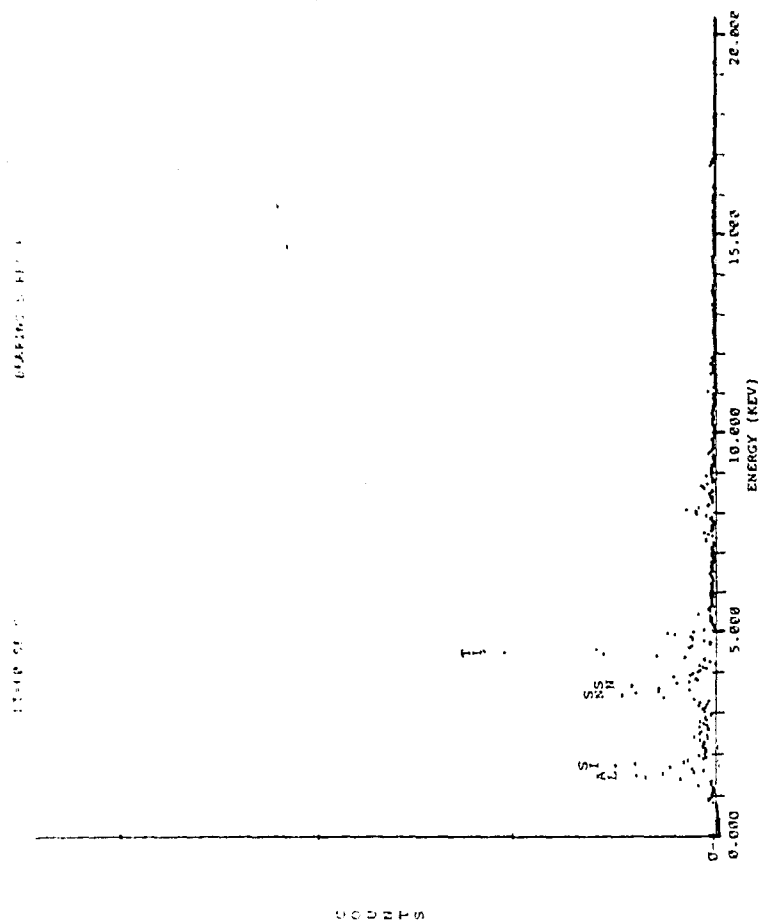
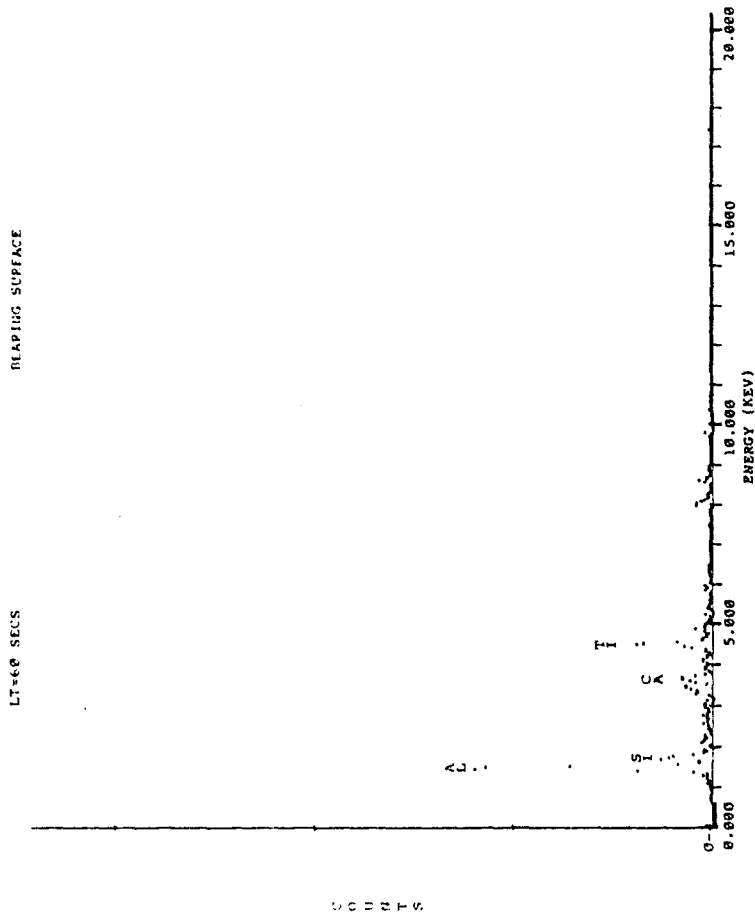


Figure 4.13c Galled Failure Zone



BEARING SURFACE

LT=60 SECS

COUNTS

AL

TI

CA

0 5.000 10.000 15.000 20.000

ENERGY (KEV)

Figure 4.13d Foreign Particle Damage

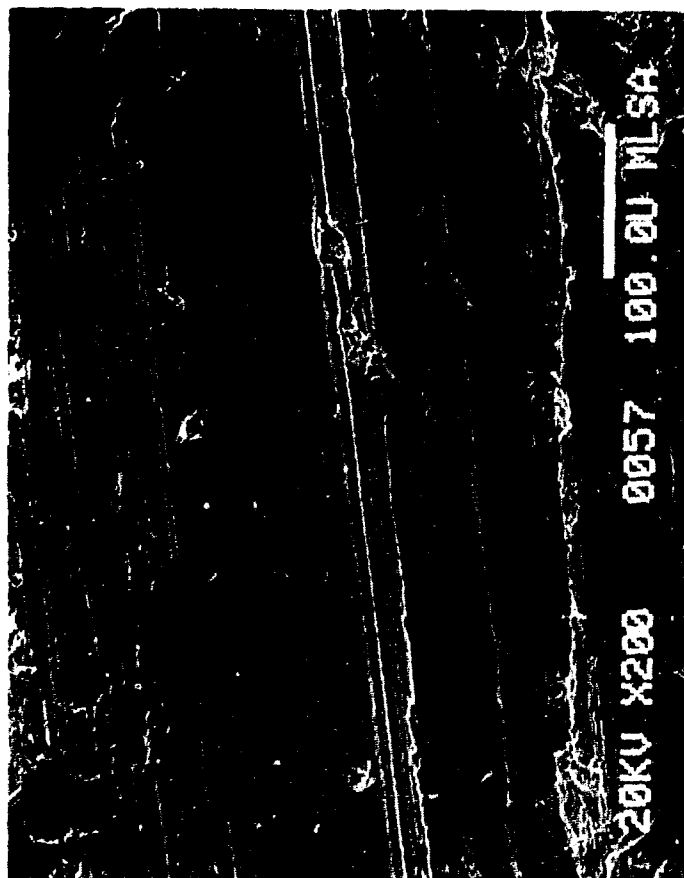
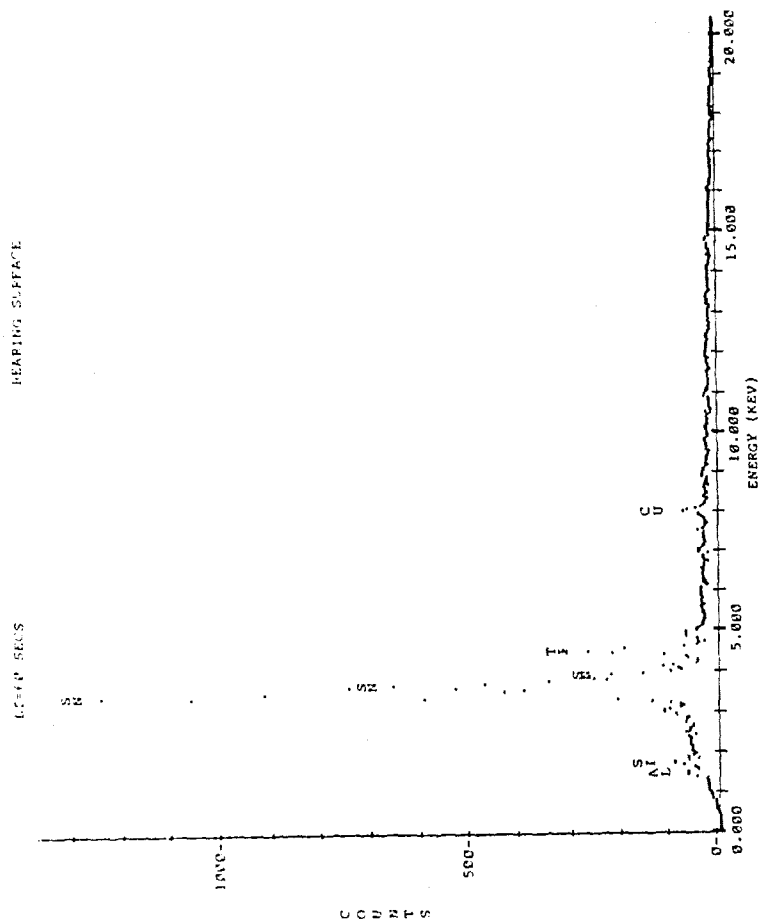


Figure 4.13e Abrasive Wear Track

The tin, aluminum, silicon, and copper peaks are sharper than in 4.13b, particularly the silicon peak. Another of the pitted areas is shown in Figure 4.13d. Aluminum, silicon, and calcium are present, a definite indication of foreign particle contamination, but no foreign particle is visible. This area is clearly visible in Figure 4.12. Figure 4.13e shows a wear track produced during the test. The wear track is 0.0028 inch wide. This wear track can be seen at the bottom center of Figure 4.12. Tin is the primary elemental component, with the elements titanium, aluminum, silicon, and copper again present.

Despite a thorough search, no embedded foreign silicon wear particles were found. Oil samples of the supply oil indicated the presence of silicon, providing a source of contamination.

2. Bench Test 2

Bench test 2 provided an indication of what the bearing should do under the conditions of the test with proper materials compatibility. The collar and babbit performed as expected and no damage was noted. As can be seen in Table I, loads were much higher than those applied in either bench tests 1 or 3, although they were much lower than the bearing should be capable of handling.

Load cell and thermocouple results are provided for comparison to the results of bench tests 1 and 3. Figure 4.14 shows the compressive load cell results. The buildup and the collapse of the compressive load that is due to lubricant film buildup can be seen in the Figure 4.15. Figure 4.16 provides the results of the thermocouples installed in the bearing pad. The sharp increases between test segments are noise spikes.

Bench test 2 used the same oil supply as bench test 1, indicating that the silicon contamination, although it certainly contributed to the bearing pad and collar failure of the first bench test, should not have attacked a proper materials choice.

3. Bench Test 3

Bench test 3 was successful in its attempt to provide a look at the failure initiation. The bench test was halted 3 minutes, 5 seconds after starting rotation of the collar. Visible damage had already occurred to the collar. After removal of the bearing pad from the holding fixture, the same black scars evident in bench test 1, indicating galling, were observed. Bearing damage did occur faster in bench test 3. This may have been due to the steel pad base.

a. Test Data Results from the compressive load cell show a pattern similar to that found in segment IV of the

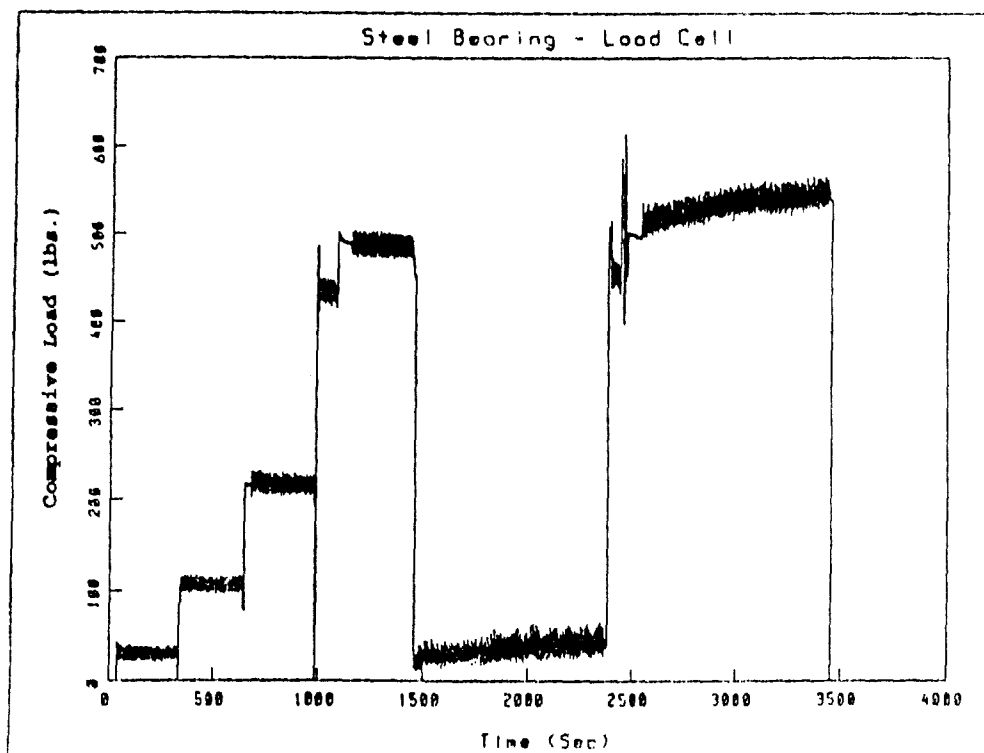


Figure 4.14 Load Cell Results - Bench Test 2

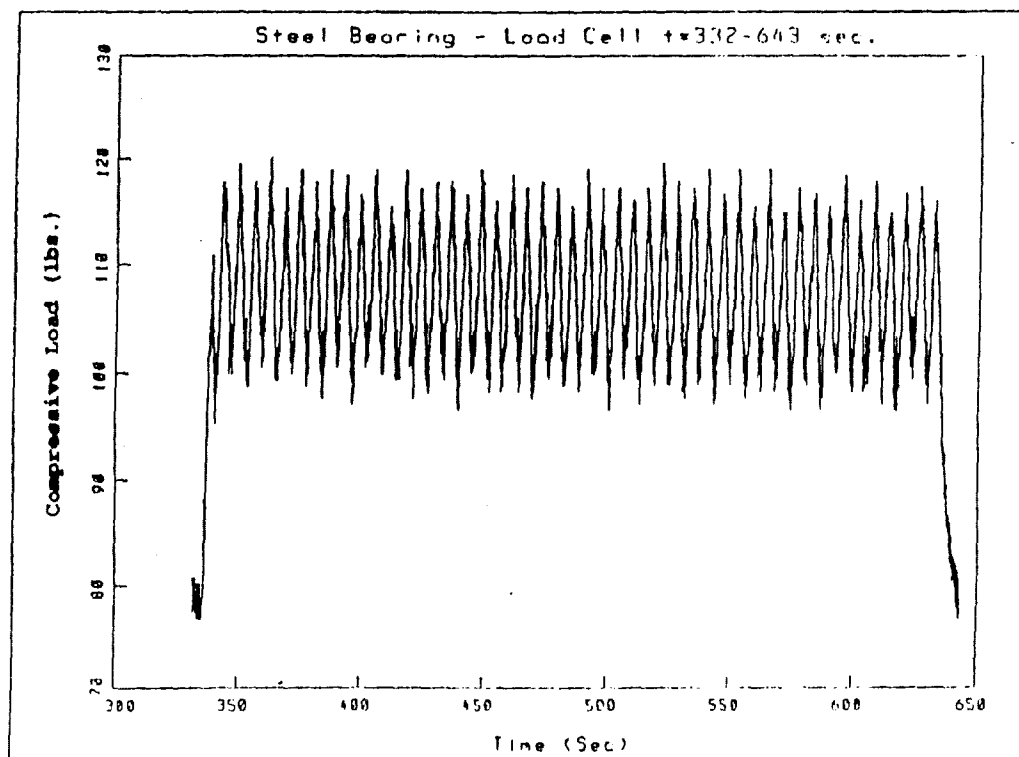


Figure 4.15 Fluid Film Development - Bench Test 2

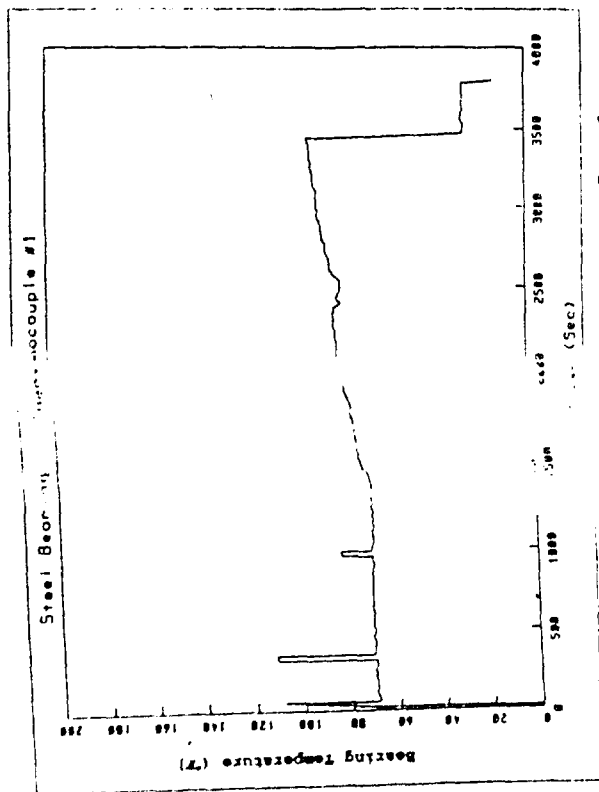


Figure 4.16a Thermocouple #1

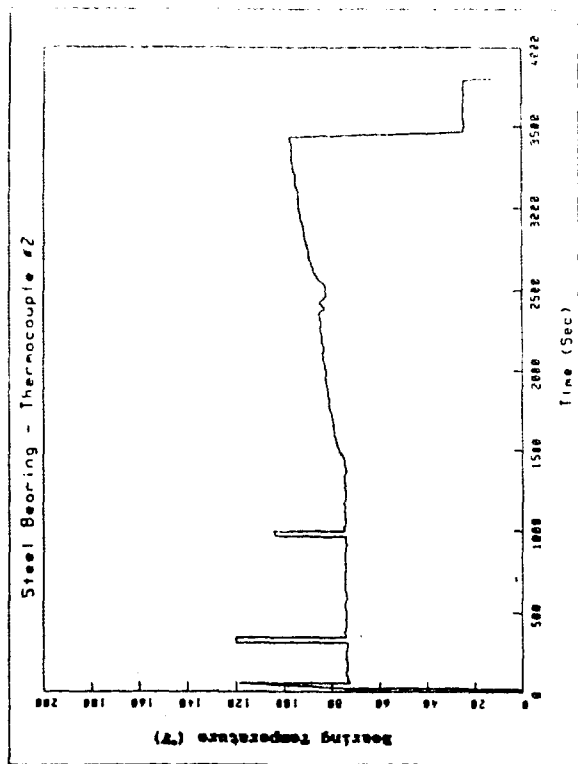


Figure 4.16b Thermocouple #2

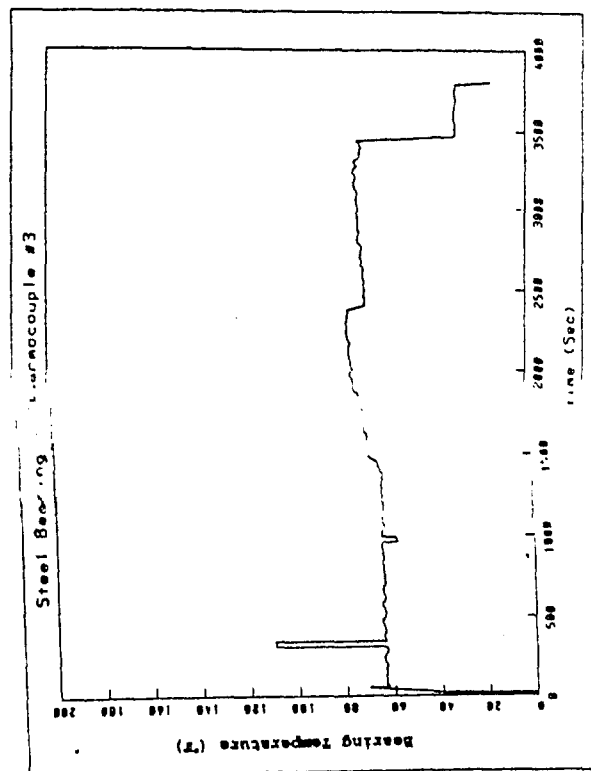


Figure 4.16c Thermocouple #3

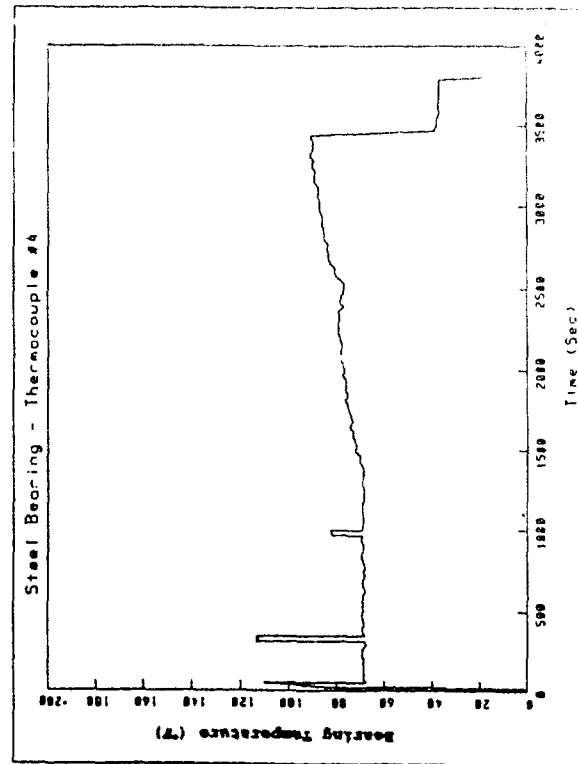


Figure 4.16d Thermocouple #4

Figure 4.16 Thermocouple Results - Bench Test 2

first bench test. Figure 4.17 shows that two load cycle frequencies are present; the frequency which matches the frequency of collar rotation owing to collar runout, and a lower frequency. When the basis for the frequency is cycles per distance slid rather than cycles per unit time, the frequency is of the same order of magnitude as the middle frequency found in test segment IV. The sharp spikes on the plot are caused by the analog tape recorder.

Frictional load measurements provided by the second load cell and the cantilever beam are presented in Figure 4.18. The results presented in Figures 4.17 and 4.18 provide a rough estimate of the friction coefficient of the material combination. The friction coefficient variation with time, and consequently distance slid, is presented in Figure 4.19. Because of the small static load applied, instrumentation noise and the limited accuracy of the load cells, the static coefficient of friction could not be determined with any confidence. However, dynamic coefficient of friction, and its variation with time and distance slid could be determined with limited confidence. The coefficient of friction reached a peak of 1.2 after 125 seconds (19.4 revolutions).

A scavenge oil sample taken at the end of the test showed 79.2 ppm of titanium, 17.6 ppm of tin, 7.6 ppm of aluminum, 0.5 ppm of copper, and 0.2 ppm of iron. This is consistent with the elements in the titanium collar and the babbitt, and does not indicate any contaminant particle introduction. A sample of the oil source taken at the end of the oil supply line indicated that the supply oil was not contaminated.

b. Visual Examination Figure 4.20 shows a photograph of the pad after testing. The wear scars are very similar to those shown in Figure 4.10b. One significant difference does exist. The wear scars in Figure 4.20 do not originate at the bearing leading edge like the majority of those in Figure 4.10b. This is discussed later in the report.

Figure 4.21 shows the collar and the pad tested in bench test 3. There are 4 radial locations of wear on the pad; however, there are only 3 radial locations of wear on the collar, indicating that the pad wore first. Large amounts of tin can also be seen on the collar on the areas where abrasive wear had not yet begun. This was not uniform circumferentially around the collar.

c. SEM and X-Ray Spectroscopy Results Cross-sectional scanning electron microscopic examination showed that the babbitt did not exhibit subsurface cracking. Depth of the wear scars was found to be 3.3 mils. Raised areas within and around the scars were also present and were of the order of 1 to 1.5 mils in height. This eliminated the possibility of babbitt fatigue.

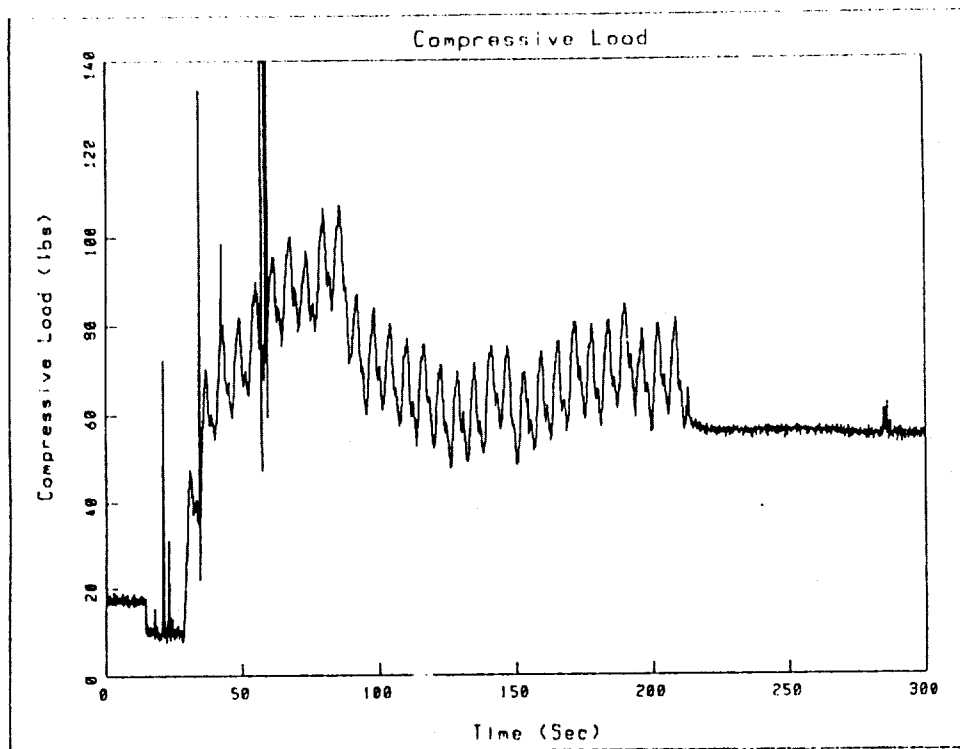


Figure 4.17 Compressive Load Results - Bench Test 3

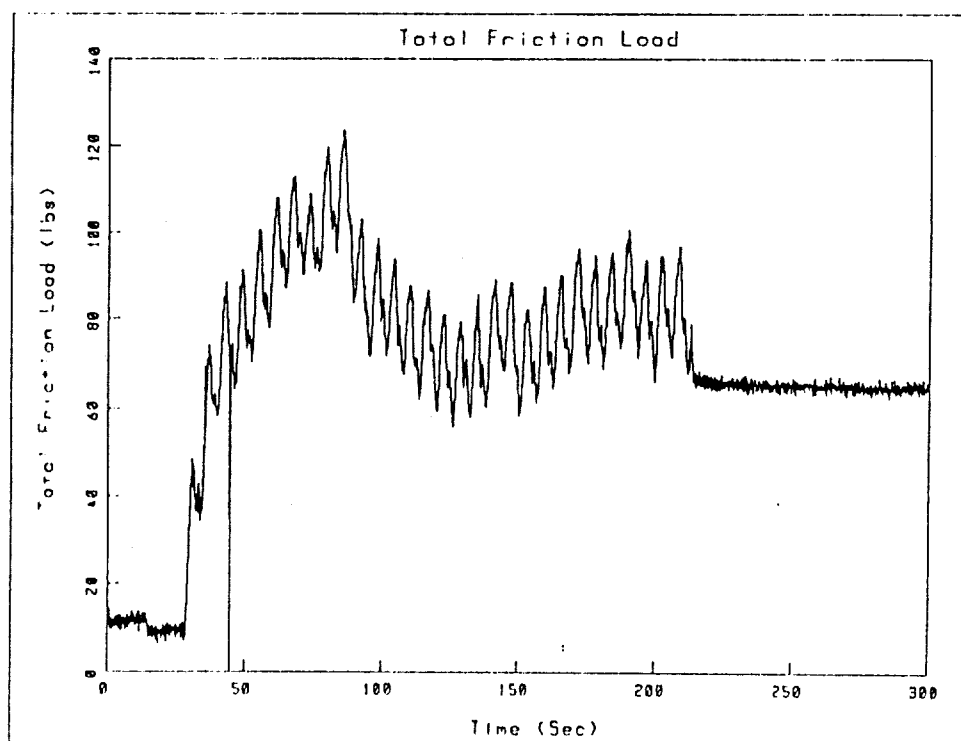


Figure 4.18 Friction Load Results - Bench Test 3

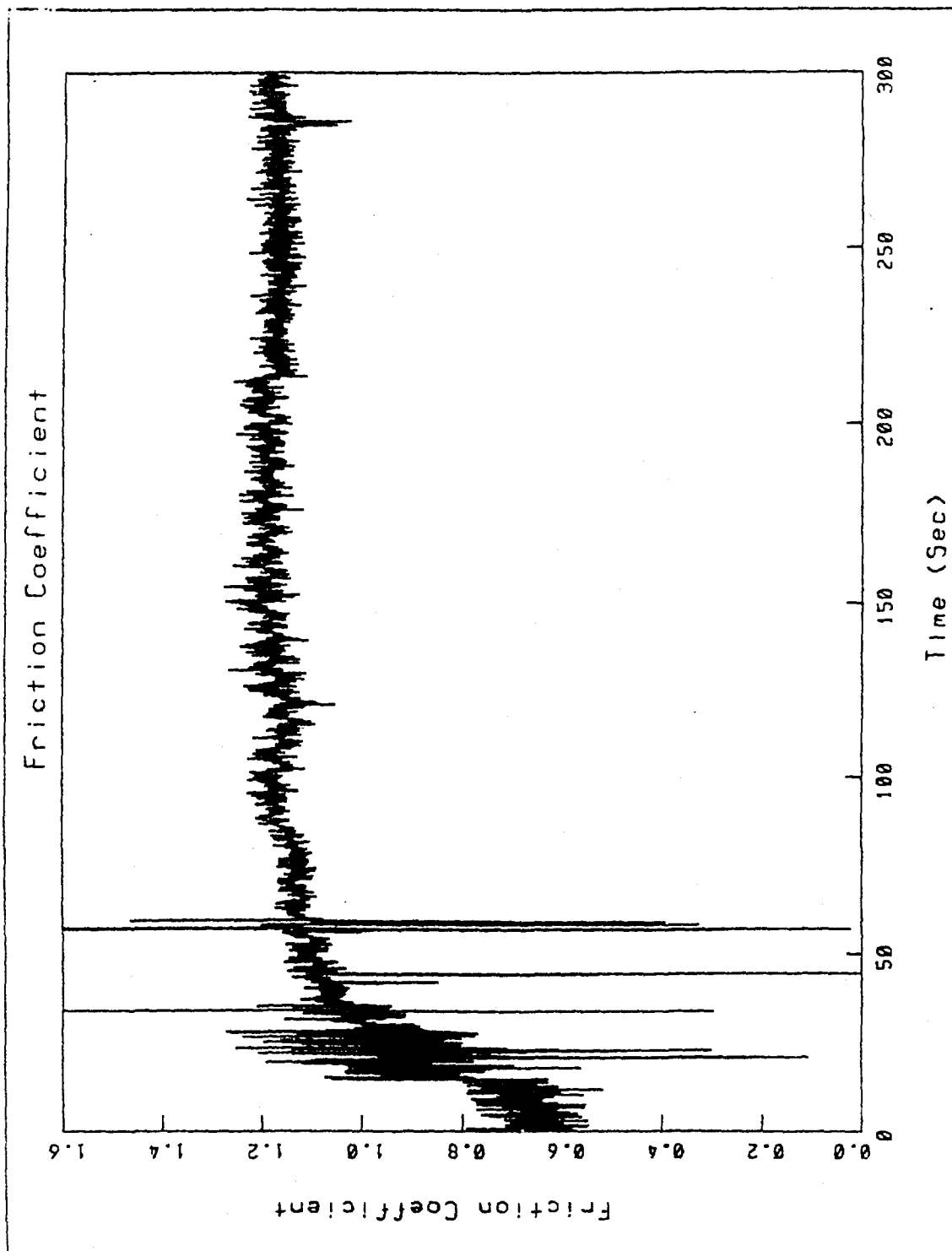


Figure 4.19 Friction Coefficient vs. Time - Bench Test 3

Figure 4.20 Bearing Pad After Bench Test





Figure 4.21 Bearing Pad and Collar After Bench Test 3

Figure 4.22 shows the SEM examination of the surface of a wear scar at its beginning and end and the corresponding elemental identification. Figure 4.22a shows the beginning of the wear scar. The direction of collar movement across the surface is upward. At the very bottom of the photograph, at the entrance to the wear scar, is a wear groove approximately 0.015 inches wide. This is indicative of a wear or foreign particle initiating the scar. Two zones are evident on the wear scar; a zone of smeared metal, followed by a zone of galling. Figure 4.22b shows a closeup of the smeared zone. Results of mass spectroscopy of the area are shown adjacent. High titanium and tin peaks are evident. Figure 4.22c shows a closeup of the galled zone. Titanium is more prevalent here than in the smeared zone. Figure 4.22d shows the scar end. There is not an exit groove for a wear particle indicating that the wear or foreign particle did not exit. No wear or foreign particle was found in the scar. The scar end is characterized primarily by galling. Figure 4.22e shows a closeup and the corresponding elemental identification. This area is identical in composition and structure to the galled zone at the scar entrance.

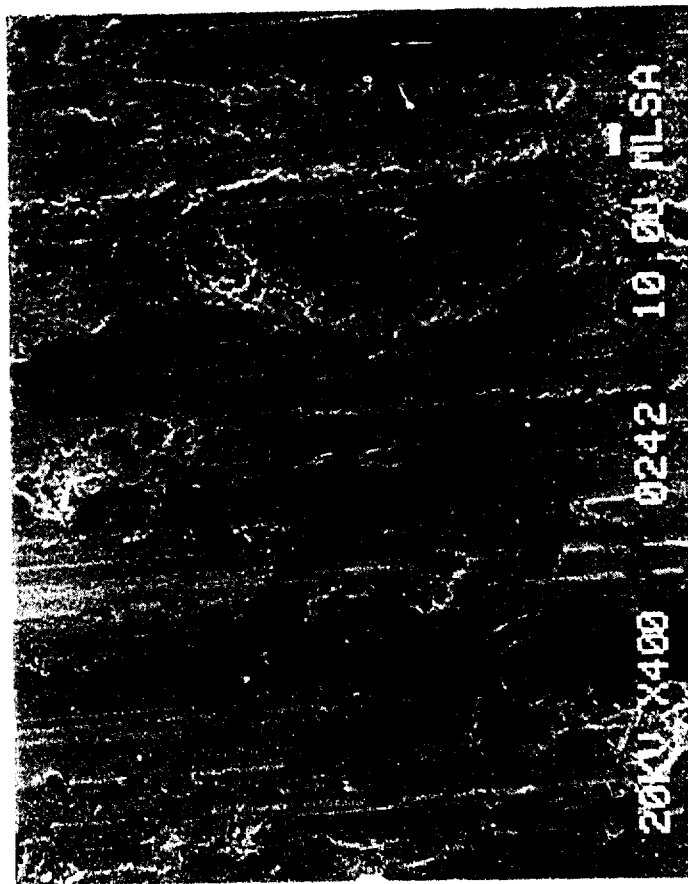


Figure 4.22a Wear Scar Beginning

Figure 4.22 SEM Photographs of Pad
After Bench Test 3

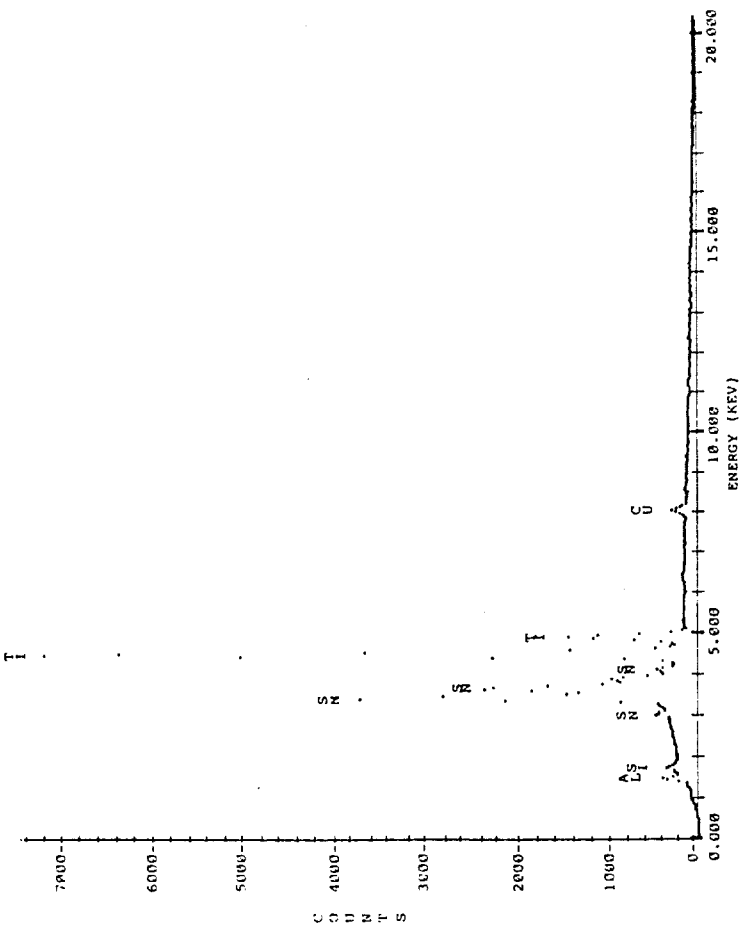
↑ Rotation

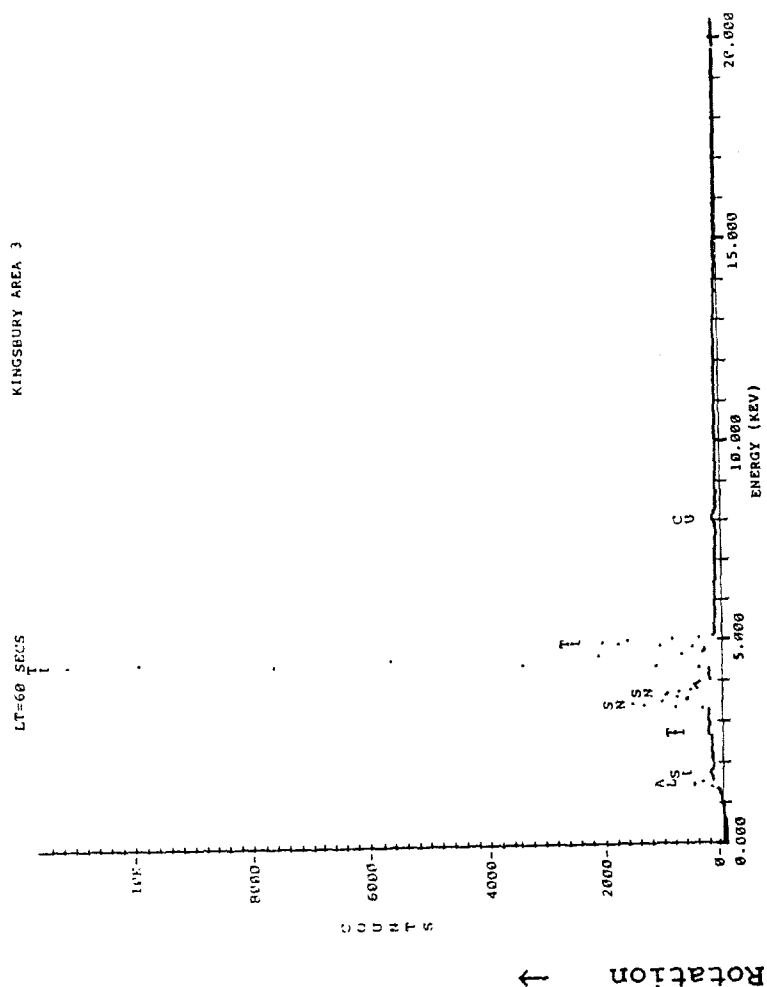
Figure 4.22b Wear Scar Beginning - Smeared Zone



KINGSBURY AREA 2

LT=60 SECS





Rotation
↑

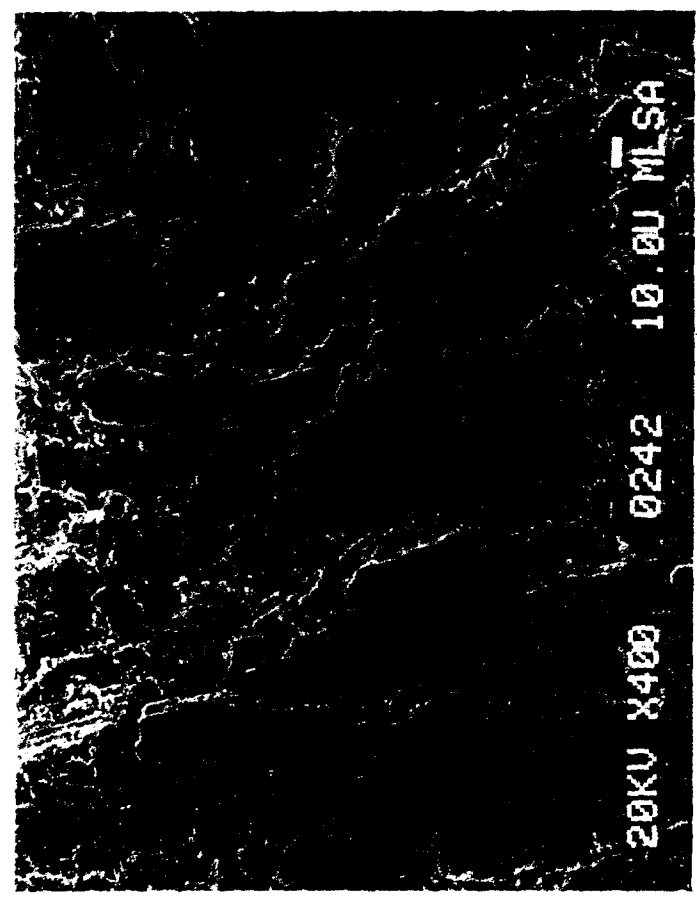


Figure 4.22c Wear Scar Beginning - Galled Zone



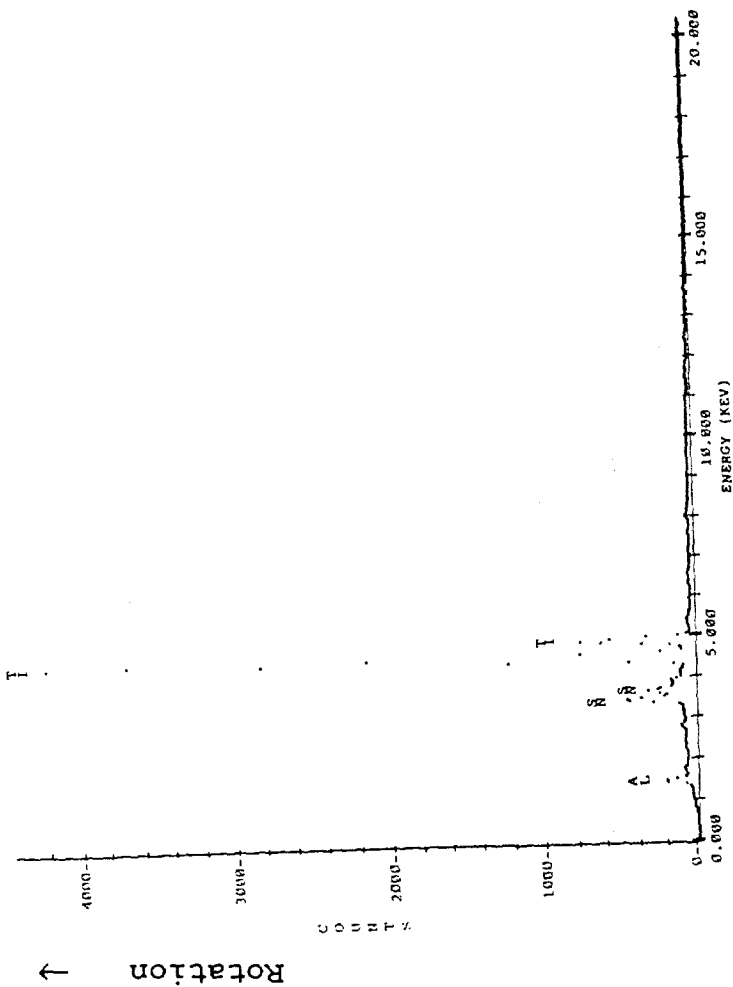
Figure 4.22d Wear Scar Exit

Figure 4.22e Wear Scar Exit - Galled Zone



KINGSBURY

LT-60 SECS



V. DISCUSSION

A. Comparison of Compressor Bearing Failure and Bench Test Results

The bench tests produced results similar to those found in the compressor bearing failure. Comparison of the compressor bearing rear pads in Figure 4.2 and the pad tested in bench test 1 in Figure 4.10c indicate similar failure modes. The three failure modes, galling, smearing, and abrasion are present in each pad.

The primary difference between the compressor bearing failure and bench tests 1 and 3 is the relative locations of the abrasive and galling failure zones. In the compressor bearing pad of Figure 4.2 the area of abrasion by wear particles precedes the area of adhesive damage and galling. In the bearing pad from the bench test, the relative locations of the areas are reversed. The pressurized oil source, leading edge groove and offset pivot of the compressor bearing would create an improved lift off of the leading edge and relatively smaller gap between pad trailing edge and collar. These conditions could not be duplicated in the bench tests and probably resulted in the differences in the relative locations of the failure mode zones.

Bearing pad temperatures achieved during the initial compressor bearing start and test segment IV of the bench tests were identical and exhibited the same patterns. This can be seen by comparing Figures 4.4b, 4.4c, and 4.4d, with Figures 4.9a, 4.9b, and 4.9d.

Oil sample results from the compressor bearing failure and the bench tests reveal significant amounts of titanium, tin, aluminum, copper and iron. However, the results of the sample from the compressor bearing failure also indicated some foreign debris. This debris was probably caused by the common oil system of the CRF drive system. The bearing oil supply was considered protected from most debris by upstream filtering but the effect of foreign debris cannot be discounted. During the low speed operation the bearing was very susceptible to usually acceptably small foreign contaminants because of the poor lubricant film thickness allowed by the titanium.

X-ray spectroscopy results of the compressor bearing rear pads and the bench test pads revealed similar results. Large amounts of titanium were found in both, indicating similar degrees of metal transfer between surfaces. The carbon found on the compressor bearing pad was probably due to the breakdown of the oil during the final stages of failure prior to compressor shutdown. The presence of alkaline metals and chlorine in the compressor bearing sample has not been explained.

B. Failure Sequence

The scenario presented for the sequence of events of the compressor bearing failure and bench tests 1 and 3 is as follows:

1. The inability of titanium to react with the lubricant provided a very thin or nonexistent lubricant film thickness. Foreign particles of a size considered acceptable for such a bearing application and small enough to avoid filtering were introduced to the bearing. Owing to the small or nonexistent film thickness, even foreign particles of a normally acceptable size were sufficient to create asperities in the babbitt. This created a small area of contact between the surfaces.

2. The two surfaces adhered at the contact points and the joints sheared, transferring material from one surface to the other and creating wear particles. Both titanium and babbitt failed in shear, primarily the babbitt. A titanium wear particle initiated galling. Titanium wear particles adhered to the babbitt and titanium collar repeatedly, creating the pad wear scars.

3. Since the lubricant film thickness was so thin, wear particles remained between the surfaces for an extended time and abrasion became the primary mechanism of wear.

4. The abrasive wear and galling continued until enough wear had occurred to allow lubricant to enter between the surfaces, washing away wear debris.

5. As debris was washed away, the surface contact increased.

6. Adhesion and abrasion created more wear debris and the cycle was repeated.

C. Supporting Evidence

This sequence of events is certainly not the only possibility, but based on the evidence gained in the bench test, is the most likely. Compressive and frictional load cell, thermocouple, oil analysis, visual and microscopic

examination, and X-ray analysis results of the surfaces all provide evidence to support this theory.

Since the relative locations of the pad and collar were fixed, increases in the compressive load indicate an increase in the gap between the pad and the collar. This increase can be a function of the film thickness or the amount of wear debris between the surfaces. Figure 4.15 shows that some lubricant film was created with the steel collar in bench test 2. At no time during bench tests 1 and 3 did any indication of an increase of load, because of lubricant film development, occur.

All of the black scars on the pad tested in bench test 1, shown after test segments IIIa and IIIb in Figure 4.10, originate at or near the pad leading edge. The first indication of the black scars, shown in Figure 4.10a, did not exhibit any evidence of large foreign contaminants. Wear of the titanium collar had begun at the same time as the development of the black scars. In bench test 3, wear grooves can be seen entering the origination point of some of the black scars in Figure 4.20. The size of the grooves may have been enlarged by wear debris carried by the collar rotation into the leading edge. It can be seen from the photograph of the pad from bench test 3 (Figure 4.20) that not all of the scars originated at a wear groove. Those that did not originate from a wear groove did originate behind another wear scar in a zone of abrasive wear. This indicates that a particle was necessary to originate the scar. This could have been a titanium wear particle or a foreign particle.

In Figure 4.20 it is shown that one area of adhesive wear is evident on the pad which did not exhibit galling. As shown in Figure 4.21, the area of the collar corresponding to this radial location did not exhibit abrasive wear. The results from bench test 1 indicate that had the test continued, galling would have developed. Also evident is the metal transfer which occurred at all radial locations of the collar. Although the results of the compressor bearing failure and bench test 1 indicate that foreign contamination was present and did contribute to the failure, bench test 3 suggests that contamination was not necessary to initiate the adhesion of the surfaces. This suggests that adhesive wear was the significant initial wear mechanism followed by galling and abrasive wear.

The load cell results show that wear debris accumulated between the surfaces. Compressive load cell results in Figures 4.5, 4.8, and 4.17 indicate an increase in load as the distance slid increased. Increases in the compressive load imply an increased distance between the surfaces as a result of the buildup of wear particles. Increases in frictional load and friction coefficient with distance slid are evident in Figures 4.18 and 4.19 respectively. Increases in friction load and friction coefficient suggest a transition from

adhesive wear to abrasive wear.

Smearing of the material on the pad is evident in the SEM results from bench tests 1 and 3. The photograph in Figure 4.22a show that the debris created by galling was carried around by the titanium collar rotation back into the scars. This debris was smeared into the scar. This may be the reason for the intermediate frequency found in test segments IV and XI, although there is not enough evidence to prove this. Other possible explanations for this intermediate frequency may lie in the removal and reconstruction of oxidized layers in the titanium, or it may be a result of the galling mechanism.

The load cell results from bench test 1, Figure 4.8a, show the buildup and washing of wear debris from the surface. This is characterized by the lowest frequency variations in the cyclic nature of compressive loading. From an initial applied load of 25 lbs, a peak load of 230 lbs was generated, followed by the washing of debris from between the surfaces. Each successive peak was smaller in magnitude indicating that more lubricant was entering after each cycle because of the asperities generated.

VI. CONCLUSIONS

The compressor bearing failure in the Wright Research and Development Center Compressor Research Facility was accurately simulated in bench tests 1 and 3. The failure was caused by two factors, both related to the selection of titanium for the thrust collar material. The first factor was the inability of the titanium to react with the lubricant selected. The second factor was the poor materials compatibility of the titanium 6-4 alloy and No. 2 babbitt. The two metals are a soluble pair which led to adhesion of the surfaces, followed by galling and abrasion by the wear particles. This was accelerated by the susceptibility of the bearing to small foreign contaminants. As the bearing was accelerated above 2½ speed, full film separation of the surfaces occurred, halting the bearing wear. Each successive start and stop increased the wear until it reached a value at which separation of the surfaces was no longer possible, resulting in catastrophic failure.

This failure and the bench tests provide supporting evidence for the adhesion theory of friction. These results are not based on ASTM test standards and only provide a cursory examination of the process.

The results of this investigation were instrumental to the successful completion of the fan rig test and a second, similar, fan rig test. The results verified that the bearing configuration with the titanium collar was unacceptable. The design of the bearing was changed, based upon the bench test results, and replaces the titanium collar with a steel collar. The first fan rig was removed, repaired, and outfitted with the steel thrust collar. While the first fan rig was being repaired, the new bearing design was successfully demonstrated on the second fan rig. This fan rig test was completed, accumulating 95 hours of operation. The bearing performed flawlessly, exhibiting no unusual wear. The first fan rig was tested with the new bearing design, resulting in 42 hours of operation, again without incident.

VII. RECOMMENDATIONS

This failure could have been avoided with a more extensive literature search or bench test prior to bearing design. A literature search would have warned of the problems associated with the choice of titanium in such an application.

Titanium was chosen for its high strength-to-weight ratio, which improved the burst characteristics of the bearing. Successful operation of the titanium collar might have been realized with the modification of the surface. One way which has been successful in reducing the wear and galling tendencies of titanium has been metal or metalloid coatings¹. The most successful coating in sliding contact has been electroless nickel¹; however, any coating would be susceptible to removal. The best solution would have been to avoid the use of titanium.

VIII. ACKNOWLEDGEMENTS

The bench tests were designed with the assistance of Mr. Fred Weisenger of Kingsbury, Inc. Instrumentation was provided by the CRF Data Group and instrumentation technicians, in particular Mr. Richard Taylor, Mr. Al Wang and Mr. Paul Dunigan. SEM examination and X-ray spectroscopy results were provided by WRDC/MLSA personnel Fred Mullins, Lee Gulley and Tom Dusz. Pratt and Whitney Corporation provided the X-ray spectroscopy results of the compressor bearing pad. All of this support is gratefully acknowledged.

IX. REFERENCES

1. Rabinowicz, E., "Frictional Properties of Titanium and Its Alloys", Metal Progress, Vol. 65, No. 2, Feb. 1954, pp.107-110
2. Miller, P.D. and J.W. Holladay, "Friction and Wear Properties of Titanium", Wear, Vol. 2, No. 2, Nov. 1958, pp. 133-140
3. Waterhouse, R.B. and M.H. Wharton, "Titanium and Tribology", Industrial Lubrication and Tribology, Vol. 26, No. 1, Jan/Feb 1974, pp.20-23